ISTANBUL TECHNICAL UNIVERSITY ★ GRADUATE SCHOOL OF SCIENCE ENGINEERING AND TECHNOLOGY

EFFECTS OF SPATIAL REGULARIZATION ON PARAMETER ESTIMATION FOR DYNAMIC PET

M.Sc. THESIS

Sahra ALAK

Department of Electronics and Communications Engineering

Telecommunication Engineering Programme

MAY 2014

ISTANBUL TECHNICAL UNIVERSITY ★ GRADUATE SCHOOL OF SCIENCE ENGINEERING AND TECHNOLOGY

EFFECTS OF SPATIAL REGULARIZATION ON PARAMETER ESTIMATION FOR DYNAMIC PET

M.Sc. THESIS

Sahra ALAK
(504111357)

Department of Electronics and Communications Engineering

Telecommunication Engineering Programme

Thesis Advisor: Assoc.Prof. Dr. Ilker BAYRAM

MAY 2014

İSTANBUL TEKNİK ÜNİVERSİTESİ ★ FEN BİLİMLERİ ENSTİTÜSÜ

UZAYSAL DÜZENLİLEŞTİRMENİN DİNAMİK PET PARAMETRE KESTİRİMLERİNE OLAN ETKİSİ

YÜKSEK LİSANS TEZİ

Sahra ALAK
(504111357)

Elektronik ve Haberleşme Mühendisliği Anabilim Dalı

Telekomünikasyon Mühendisliği Programı

Tez Danışmanı: Doç. Dr. Ilker BAYRAM

MAYIS 2014

Sahra Alak, a **M.Sc.** student of ITU **Graduate School of Science Engineering and Technology** student ID **504111357**, successfully defended the **thesis** entitled "**EFFECTS OF SPATIAL REGULARIZATION ON PARAMETER ESTIMATION FOR DYNAMIC PET**", which she prepared after fulfilling the requirements specified in the associated legislations, before the jury whose signatures are below.

Thesis Advisor :	**Assoc. Prof. Ilker BAYRAM** İstanbul Technical University	.....
Jury Members :	**Assoc. Prof. Mustafa Ersel KAMASAK** İstanbul Technical University	.....
	Assist. Prof. Dr. Gökhan Bilgin Yildiz Technical University	.....

Date of Submission : 02 May 2014
Date of Defense : 29 May 2014

To my family,

FOREWORD

I would like to thank Assoc. Prof. Dr. Mustafa E. Kamaşak, Assoc. Prof. Dr. Ilker Bayram. I like to give my special thanks to my family for their neverending support and encouragement.

May 2014 Sahra ALAK
(Electrical-Electronics Engineer)

TABLE OF CONTENTS

Page

FOREWORD ..... **ix**
TABLE OF CONTENTS ..... **xi**
ABBREVIATIONS ..... **xiii**
LIST OF TABLES ..... **xv**
LIST OF FIGURES ..... **xvii**
SUMMARY ..... **xix**
ÖZET ..... **xxi**
1. INTRODUCTION **1**
1.1 Pozitron Emission Tomography 3
1.2 Compartmental Models 6
1.3 Kinetic Parameter Estimation With Spatial Regularization 9
2. METHOD **15**
3. RESULT **19**
4. DISCUSSION **41**
5. CONCLUSION **43**
REFERENCES **45**
CURRICULUM VITAE **49**

ABBREVIATIONS

AWGN	**:** Additive White Gaussian Noise
BG	**:** Background
CT	**:** Computed Tomography
FDG	**:** Florodeoksiglukoz
HR	**:** High Spatial Regularization
KM	**:** Kinetic Modeling
LR	**:** Low Spatial Regularization
MR	**:** Medium Spatial Regularization
MRI	**:** Magnetic Resonance Imaging
NEE	**:** Noise Based Estimation Error
NR	**:** No Spatial Regularization
ODE	**:** Order Differential Equation
PET	**:** Positron Emission Tomography
REE	**:** Regularization Based Estimation Error
ROI	**:** Region of Interest
SNR	**:** Signal To Noise Ratio
TAC	**:** Time Activity Curve

LIST OF TABLES

Page

Table 1.1: Pozitron Emitter Radionuclides and Their Clinical Uses 5
Table 2.1: Kinetic Parameter Values in simulations 16
Table 3.1: Results of Bias, CV and MSE for ROI 2 of k1 parametric images with different spatial regularization 35
Table 3.2: Results of Bias, CV and MSE for ROI 2 of k2 parametric images with different spatial regularization 36
Table 3.3: Results of Bias, CV and MSE for ROI 2 of k3 parametric images with different spatial regularization 37
Table 3.4: Results of Bias, CV and MSE for ROI 2 of k4 parametric images with different spatial regularization 38
Table 3.5: Results of Bias, Variance and MSE for ROI 1 of k1 parametric image .. 38
Table 3.6: Results of Bias, Variance and MSE for ROI 1 of k2 parametric image .. 39

LIST OF FIGURES

Page

Figure 1.1 : PET Imaging Sytems [25] 4
Figure 1.2 : One Tissue Compartmental Model 7
Figure 1.3 : Two Tissue Compartmental Model 9
Figure 1.4 : M-Estimators 13
Figure 2.1 : Phantom Image 15
Figure 2.2 : Dynamic sequence of a slice of a phantom image 16
Figure 2.3 : Noiseless TAC for two different foreground regions 17
Figure 3.1 : Noisy images of time frame 12 of dataset at different SNR values 19
Figure 3.2 : Parametric images of k1, k2, k3 and k4 estimated by NR, LR, MR and HR for 0.5 dB SNR value 21
Figure 3.3 : Parametric images of k1, k2, k3 and k4 estimated by NR, LR, MR and HR for 1 dB SNR value 22
Figure 3.4 : Parametric images of k1, k2, k3 and k4 estimated by NR, LR, MR and HR for 4 dB SNR value 23
Figure 3.5 : Parametric images of k1, k2, k3 and k4 estimated by NR, LR, MR and HR for 8 dB SNR value 24
Figure 3.6 : Parametric images of k1, k2, k3 and k4 estimated by NR, LR, MR and HR for 10 dB SNR value 25
Figure 3.7 : Parametric images of k1, k2, k3 and k4 estimated by NR, LR, MR and HR for 20 dB SNR value 26
Figure 3.8 : 64th row of profile obtained parametric images with different spatial regularization for 0.5 dB SNR. Parametric images with original, LR, MR and HR are plotted using yellow, blue, cyan and red colors respectively 27
Figure 3.9 : 64th row of profile obtained parametric images with different spatial regularization for 1 dB SNR. Parametric images with original, LR, MR and HR are plotted using yellow, blue, cyan and red colors respectively 28
Figure 3.10 : 64th row of profile obtained parametric images with different spatial regularization for 4 dB SNR. Parametric images with original, LR, MR and HR are plotted using yellow, blue, cyan and red colors respectively 29
Figure 3.11: 64th row of profile obtained parametric images with different spatial regularization for 8 dB SNR. Parametric images with original, LR, MR and HR are plotted using yellow, blue, cyan and red colors respectively 29
Figure 3.12 : 64th row of profile obtained parametric images with different spatial regularization for 10 dB SNR. Parametric images with original, LR, MR and HR are plotted using yellow, blue, cyan and red colors respectively 30

Figure 3.13 : 64th row of profile obtained parametric images with different spatial regularization for 20 dB SNR. Parametric images with original, LR, MR and HR are plotted using yellow, blue, cyan and red colors respectively 30
Figure 3.14 : Comparison of the Mean Square Error Analysis for k1 image with different spatial regularization and SNR values. Parametric images with LR, MR and HR are plotted using blue, cyan and red colors respectively 31
Figure 3.15 : Comparison of the Mean Square Error Analysis for k2 image with different spatial regularization and SNR values. Parametric images with LR, MR and HR are plotted using blue, cyan and red colors respectively 32
Figure 3.16 : Comparison of the Mean Square Error Analysis for k3 image with different spatial regularization and SNR values. Parametric images with LR, MR and HR are plotted using blue, cyan and red colors respectively 33
Figure 3.17 : Comparison of the Mean Square Error Analysis for k4 image with different spatial regularization and SNR values. Parametric images with LR, MR and HR are plotted using blue, cyan and red colors respectively 34

EFFECTS OF SPATIAL REGULARIZATION ON PARAMETER ESTIMATION FOR DYNAMIC PET

SUMMARY

Positron emission tomography (PET) is a medical imaging modality that allows a powerful tool for clinical diagnosis of various diseases such as cancer, tumor detection, epilepsy, coronary artery, parkinson and alzheimer. Furthermore, PET offers the mapping of in vivo neurobiological functions such as metabolism, blood flow, enzyme activity, and neuroreceptor binding site density and occupancy.

Among several imaging modalities (such as MRI, SPECT, optical imaging) for molecular imaging, PET imaging has several advantages such as high sensitivity and ability for quantitative measurement. Quantification of the biochemical process of interest targeted by the radiotracer is done by analyzing the PET emission data as a function of time. PET emission data is formed into various time frames and reconstructed to obtain PET image data which represents the radiotracer distribution in tissue at specific time points. Development and progress phases of the tissue with disease can be diagnosed after all the tissues are scanned by the radiotracer.

A typical PET study is based on physical properties of the radiotracer which is known as a positron emitting radionuclide. PET radiotracers are injected in very small quantities. Radionuclide is emitting positron to be stable. The tracer decays by emitting a positron which annihilates with an electron and produces a pair of annihilation 511 KeV photons moving in opposite directions. Some of the emitted photons are then collected by the detectors of a PET scanner and turn into images using computers which have related software.

PET image can be acquired with two main types of acquisition, static and dynamic. Depending on the application, images are measured to count the activity of the tracer over a single fixed period. This procedure is called static PET imaging. On the other hand, the activity of the tracer can be measured for each voxel at different time periods. Such prosedure is called dynamic PET imaging. The graphic that shows the change of the tracer's density in the tissue with time is called time activity curve (TAC). TACs can be generated by defining regions of interest (ROIs) and sampling the image over all time frames.

The main problem in dynamic PET imaging is dividing the signals into time intervals. If the signals are divided into small intervals, signal to noise ratio is decreased in every interval. On the other hand, longer time intervals cause higher signal to noise ratio but the resolution of reconstructed images decreases. Therefore, determination of time intervals is important for the resolution of the images. Images are reconstructed in short time interval just after the injection of the tracer. Since the pace of the tracer in tissue decreases with time, time intervals increase after a while. Psychological parameters are evaluated by modelling TACs. The most common modelling type is comportment models.

Different comportment models can be used according to complexity of the tissue is psychology. The purpose of the comportment models is to give information about the status of the tracer in different chemical situations or in different place like plasma, tissue, etc. It also informs about the speed of the tissues transmit from one medium to another transmit the speed between different mediums is described with kinetic parameters.

In this thesis, a comportment model with two tissues is used which is suitable for raclopride tracer. In this comportment model, C_P comportment shows the density of tracer in plasma and it is measured from plasma samples which are taken from artery vessels. C_{T1} comportment demonstrates the tracer density that is not metabolized in the tissue whereas C_{T2} comportment shows the tracer destiny that is metabolized. In this model, there are four types of kinetic parameters k_1, k_2, k_3 and k_4 parameters show the speed of tracer from plasma to tissue, from tissue to plasma, metabolism speed and dematobolism speed respectively. k_1, k_2, k_3 and k_4 can be calculated with the help of tracer density in plasma, the tracer's total density in plasma and tissues.

Phantom image with resolution of 128x128 pixels which has two different region of interest is constructed by using MATLAB program. TACs are obtained by sampling the images in ROI's. Four different original images are developed according to kinetic parameters taken from literature. Time intervals used in simulations are 4x0.5, 4x2 and 10x5 minutes with total 18 frames and 60 minutes duration. Since transition of the tracer in the tissue is faster at the beginning, initial time intervals are taken as small. On the other hand, time intervals are taken larger after since the transition becomes slower.

By combining all the values of one pixel at different time points TAC are evaluated. Noise by using AWGN function of MATLAB is added to the TAC which is developed from kinetic parameters. Added SNR valuves are 0.5, 1, 4, 8, 10 and 20 dB.

Kinetic parameter estimation of spatial regularization is not worked frequently in the literature. This work proposes a solution for different noise values according to the effects of spatial regularization on parametric images. The purpose of thesis is to provide parametric images with the help of kinetic parameter estimation after the spatial regularization parameters are analyzed.

Simulations results of parametric images are obtained by using four different spatial regularization methods in order to evaluate the performance of the developed algorithm. Simulations are run by using four different spatial regularization methods as no, low, medium and high spatial regularization. Analysis of parametric images shows that proper selection of the regularization parameters is important for dynamic PET. These parameters are found for the each spatial regularization method after experimental work. The kinetic parameters are estimated for each pixel, and the estimated kinetic parameters form "parametric images".

MATLAB simulations show that the proposed method anticipates the correct changes like the functions of spatial regularization. The best estimation method by using TAC and the model result is to minimize MSE between TAC and the model.

UZAYSAL DUZENLİLEŞTİRMENİN DİNAMİK PET PARAMETRE KESTİRİMLERİNE OLAN ETKİSİ

ÖZET

Pozitron emisyon tomografisi (PET) tıbbi alanda kullanılan ve pozitron yayıcı radyonüklidlerin insan vücudundaki dağılımını üç boyutlu (tomografik) olarak görüntüleyen tanısal bir nükleer tıp yöntemidir. Kanser, tümör, epilepsi, koroner arter, parkinson ve alzheimer gibi çeşitli hastalıkların klinik tanısında kullanılır. Biyokimyasal, metabolik veya fonksiyonel parametrelere göre farklı radyofarmasötikler kullanılır ve in-vivo olarak görüntülenir. Doku perfüzyonu, oksijen kullanımı, glikoz metabolizması, nükleik asit metabolizması ve östrojen reseptör dağılımı PET ile ölçülebilen ve en yaygın kullanılan parametrelerdir.

Diğer moleküler görüntüleme teknikleri (MRI, optik görüntüleme, SPECT) ile karşılaştırıldığı zaman PET yüksek hassasiyet ve nitelikli ölçüm yaptığı için birçok avantaj sağlamaktadır. PET bir çok patofizyolojik durumda yapısal bozuklukların oluşmadığı, erken dönemde oluşan biyokimyasal ve metabolik değişiklikleri tespit ederek erken tanıya olanak sağlar. PET emisyon verileri çeşitli zaman çerçevelerinde oluşturulur ve doku içerisindeki izleyicinin dağılımı belirli zaman dilimlerinde ölçülüp haritalandırılır. Düşük radyasyon içeren izleyici ile bütün dokular taranıp, hastalıklı hücrenin oluşum, gelişim ve ilerleme süreci tespit edilir. PET görüntüsünün bir diğer avantajı ise dokunun kesitler halinde görüntülenebilmesidir. Bu sayede bir organın neredeyse tamamının radyoizotop etkisi altında davranışını görüntüleyebilme kabiliyetine sahiptir.

PET'in çalışma prensibi pozitron yayıcıları olarak bilinen belli radyoaktif izotopların fiziksel özelliklerine dayanır. Radyoaktif çekirdek kararlı hale geçmek için çekirdekten pozitron saçılımı gerçekleştirir. Pozitron ortamda kısa bir mesafe ilerledikten sonra başka bir atomun elektronuyla (negatif yüklü) çarpıştıklarında kütlenin enerjiye dönüşümü olayı gerçekleşir. Çarpışan partiküllerin kütleleri yok olurken, 511 keV (kiloelektron volt) enerjili iki tane annihilasyon fotonu birbiriyle 180 derece açı yaparak zıt doğrultuda salınır. Bu olaya annihilasyon (yok olma) denir. Pozitron yayıcılar radyonüklidlerin yaydığı ışınları özel dedektörler yardımıyla alarak, gelişmiş yazılımları olan bilgisayarlar aracılığı ile görüntülere dönüştürülür. Oluşan görüntü, radyoaktif özelliğe sahip maddenin, dokunun içerisinde hangi kimsayallarla reaksiyonlara girdiği, hangi vücut bölgelerine gönderildiği, hangi dokularda parçalandığı gibi fizyolojik doku bilgilerini gösterir.

Radyonüklitler, pozitron yayan radyoaktif maddelerdir ve birleşerek radyofarmasötikleri oluşturur. PET görüntülemede kullanılan radyofarmasötik ve radyonüklidlerin en önemli özelliği vücudun temel altyapı taşları olan Karbon (C), Oksijen (O), Flor (F) ve Azot (N) gibi elementleri içermeleridir. Böylece kullanılan işaretli molekül vücutta ilgili fizyolojik ve metabolik yollara girerek moleküler düzeyde görüntülemeye olanak sağlar. En sık kullanılan pozitron yayıcı radyonüklidler Flor (^{18}F), Oksijen (^{15}O), Nitrojen (^{13}N) ve Karbon (^{11}C)'dir.

Günümüzde en yaygın olarak kullanılan PET radyofarmasötiği [^{18}F] Florodeoksiglukoz (FDG)'dur. FDG yapısal ve biyokimyasal davranış olarak glukoza çok benzerdir. FDG bir glikoz analoğudur ve onkolojik çalışmalarda kullanılmaktadır. Bu çalışmada beyin fonksiyonlarını incelemeye yardımcı olan dopamin molekülünün miktarı rakloprid [^{11}C] izleyicisi yardımıyla tespit edilir. Dopamin, normal olarak beyin hücrelerinde bulunan ve hücreler arası iletişimde rol oynayan bir moleküldür. Bu molekülün eksikliği ya da fazlalığında çeşitli hastalıklara yol açmaktadır. Örneğin Parkinson hastalığında dopamin beyinde yetersiz miktarda bulunur. Ayrıca, PET sayesinde beyindeki hangi hücrelerin epilepsiye sebep olduğu anlaşılmaktadır.

PET görüntüleri uygulamaya bağlı olarak statik veya dinamik olarak elde edilir. Durağan (statik) PET görüntüleme yöntemi, izleyicinin canlı içerisindeki son durumdaki dağılımı göstermek için kullanılır. Değişken (dinamik) PET görüntüleme yönteminde ise izleyicinin canlı içerisindeki aktivitesini belirli zaman aralıkları ile gözlemleyerek dağılım süreci görüntülenmek istenir. Bu sayede fizyolojisi hakkında bilgi sahibi olunur. Dağılım sürecini gözlemleyebilmek için canlıya izleyici enjekte edilir ve sinyaller enjekte edildiği andan itibaren kayıt altına alınır. Elde edilen bütün sinyaller zaman aralıklarına bölünerek, her zaman aralığı için görüntüler elde edilir.

Dinamik PET görüntülemedeki en önemli problem toplanan sinyallerin zaman aralıklarına bölünmesindedir. Kısa aralıklara bölünen sinyaller, her zaman aralığındaki sinyal-gürültü oranının düşmesine sebep olmaktadır. Zaman aralıklarının büyütülmesi sinyal-gürültü oranının artmasına sebep olur fakat elde edilen görüntülerdeki çözünürlük azalmaktadır. Bu yüzden zaman aralıklarının belirlenmesi görüntülerin çözünürlüğü ve doğru tespiti için önem taşımaktadır. İzleyici enjekte edildikten hemen sonra dağılımın hızlı değişeceği tahmin edildiği için, görüntü kısa zaman aralıkları ile kayıt edilir. Daha sonra izleyicinin doku içerisindeki dağılım hızı azalacağından dolayı zaman aralıkları büyütülür.

Dokuya enjekte edilen izleyicinin yoğunluğunun zaman içerisindeki değişiminin ölçüldüğü grafiğe zaman-aktivite eğrisi (TAC) adı verilmektedir. Zaman aktivite eğrilerini kullanıp uygun şekilde modelleyerek fizyolojik parametreler hesaplanır, bu parametrelere bakarak canlı fizyolojisi hakkında bilgi sahibi olunur. Parametreleri hesaplamak için kullanılan en yaygın model türü kompartıman modelleridir.

Dokunun fizyolojisinin karmaşıklığına bağlı olarak farklı kompartıman modelleri kullanılır. Kompartıman modellerinin amacı izleyicinin farklı kimyasal durumlardaki (metabolize edilmiş, metabolize edilmemiş vs.) veya izleyicinin farklı yerlerdeki (plazma, doku vs.) durumu ve izleyicinin ortamlar arasındaki geçiş hızları hakkında bilgi sahibi olmamızı sağlar. Kompartımanlar arasındaki izleyicinin geçiş hızı kinetik parametrelerle ifade edilmektedir.

Bu tezde kullanılan raclopride (^{11}C) izleyicisine uygun olan iki dokulu kompartıman modeli kullanılmıştır. Kullanılan kompartıman modelde C_P kompartıman plazma içerisindeki izleyici yoğunluğunu göstermekte olup canlının atar damarlarından alınan plazma örneklerinden ölçülmektedir. C_{T1} kompartıman doku içerisinde metabolize edilmemiş izleyici yoğunluğunu, C_{T2} kompartıman ise doku içerisinde metabolize edilmiş olan izleyici yoğunluğunu göstermektedir. Bu modelde dört tane kinetik parametreler bulunmaktadır. k_1 kinetik parametresi plazmadan dokuya geçen izleyicinin geçiş hızını, k_2 kinetik parametresi dokudan plazmaya geçen izleyicinin geçiş hızını, k_3 kinetik parametresi dokuda metabolizma olan izleyicinin metabolizasyon hızını, k_4 kinetik parametresi ise dokuda metabolizma olan

izleyicinin de-metabolizasyon hızını göstermektedir. Plazma icerisindeki izleyici yoğunluğu (C_P), plazma ve dokulardaki izleyicinin toplam yoğunluğu bilinmesi sayesinde kinetik parametreler olan k_1, k_2, k_3 ve k_4 dolaylı kestirim ile kinetik parametreler hesaplanır.

Bu çalışmada iki farklı ilgili bölgeye (region of interest, ROI) sahip çözünürlüğü 128 × 128 pixel olan phantom imgesi MATLAB programı kullanılarak oluşturuldu. Zaman aktivite eğrileri ROI tanımladıktan sonra görüntüler bu alanda örnekleyerek elde edildi. Literatürden alınan kinetik parametrelere göre 4 farklı orjinal imgeler elde edilmiştir. Bu imgeler oluşturulurken büyük yarıçapa sahip bölgenin kinetik parametrelerinin değerleri k_1 = 0,1836, k_2 = 0,8968, k_3 = 0, k_4 = 0 kullanılırken küçük yarıçapa sahip bölgenin kinetik parametrelerinin değerleri k_1 = 0,0918, k_2 = 0,4484, k_3= 1,2408, k_4 = 0,1363'tür. Benzetimlerde kullanılan zaman aralıkları ise 4x0,5 dakika, 4x2 dakika ve 10x5 dakika olup, toplamda 18 zaman aralığı ve toplam süre 60 dakika olmaktadır. Izleyicinin doku içerisinde yayılımı hızlı olduğu için ilk zaman aralıkları daha kısa periyotlarla ölçülmüştür, daha sonraki aralıklar izleyicinin doku içerisindeki yayılımı yavaşladığı için daha uzun sürelerle ölçümler yapılmıştır.

Oluşturulan iki farklı bölgenin belirli bir pikselin tüm zamandaki değerleri birleştirilerek o piksele ait zaman aktivite eğrisi elde edilmiştir. Bu kinetik parametrelerin oluşturduğu zaman-aktivite eğrisinin üzerine MATLAB'in toplanır beyaz gauss gürültüsü fonksiyonu kullanılarak gürültü eklenmiştir. Eklenen sinyal gürültü oranları sırasıyla 0,5 dB, 1 dB, 4 dB, 8 dB, 10 dB ve 20 dB'dir. Bu çalışmada her gürültülü değerleri için oluşturulan imgeler için kinetik parametre tahmininin farklı uzaysal regülarizasyon etkileri araştırılmıştır.

Uzaysal regülarizasyonlar üzerindeki kinetik parametre tahmini yöntemi şimdiye kadar literatürde fazla araştırılmış bir yöntem değildir. Bu çalışma parametrik görüntülerde uzaysal regülarizasyonunun etkileri incelenip farklı gürültü seviyeleri için uygun bir çözüm sunmaktadır. Tezin amacı, çeşitli gürültü seviyeleri için farklı uzaysal regularizasyon parametrelerini inceleyerek kinetik parametreler kestirilerek parametrik görüntüler oluşturmaktır.

Bu tezde oluşturulan her gürültülü imgeleri için kinetik parametre tahmininin uzaysal regülarizasyonda etkileri araştırılmıştır. Geliştirilen algoritmanın performansını değerlendirmek amacıyla, dört farklı uzaysal regülarizasyon kullanılarak parametrik görüntüler benzetim sonuçları elde edilmistir. Uzaysal regülarizasyon uygulanmayan (NR), düşük uzaysal regülarizasyonu (LR), orta uzaysal regülarizasyonu (MR), yüksek uzaysal regülarizasyonu (HR) olmak uzere dört farklı uzaysal regülarizasyon parametreleri kullanılarak simülasyonlar yapılmıştır. Deneysel çalışmalardan sonra, her uzaysal regularizasyon türü için en iyi parametre değerleri bulunmuştur. Farklı miktarlarda uygulanan uzaysal regülarizasyonlar ile tüm piksellere ait kinetik parametreler kestirilerek parametrik görüntüler oluşturuldu.

Oluşan parametrik görüntülerden yanlılık (bias), varyans katsayısı (coefficient of variance) ve ortalama karesel hata (MSE) gibi istatiksel değerler farklı gürültü seviyeleri, iki farklı ilgili bölge ve dört farklı regülarizasyon parametreleri için bu değerler hesaplandı. Elde edilen zaman aktivite eğrisi ile model çıktısı kullanılarak hesaplanan bu değerleri en aza indirecek kinetik parametreleri bulmaktır. Gürültüye ve ya regülarizasyona dayalı kestirim hatalarına bakılarak çeşitli gürültü seviyelerinde ve farklı ilgili bölgeye göre uygun uzaysal regülarizasyon parametresinin bulmayı amaçlamaktadır.

1. INTRODUCTION

Nuclear medicine is a a field of medical imaging which assists the potential identification of several diseases such as heart disease, gastrointestinal, endocrine, neurological disorders, many types of cancers, and other abnormalities by detecting molecular activity within the body. Unlike anatomical based imaging techniques such as magnetic resonance imaging (MRI) and X-ray computed tomography (CT), positron emission tomography (PET) is a radiotracer functional imaging technique, which allows in vivo visualization of biochemical and physiological processes [1]. These procedures small amounts of use radioactive material in order to detect several diseases at early stages and observe the patient's responses to the treatment. PET imaging differs itself from other imaging modalities by high sensitivity and quantitative measurement possibility. Several diseases including cancer, brain disorders, heart conditions and others can be detected via PET scans very effectively. Besides, various body functions that are crucially important in detecting, treating, and monitoring diseases are measured by PET imaging. These body functions include blood flow, oxygen use, and glucose metabolism rate. Their measurement helps physians to evaluate the functioning of organs and tissues.

Static PET imaging is started a certain period of time after radiotracer injection and the activity concentration of the radiotracer is measured over a fixed period of time. Dynamic positron emission tomography provides the additional temporal information of tracer kinetics compared to static PET. Dynamic PET imaging, activity of the radiotracer can be measured at multiple time points and this activity concentration plotted versus time to form time activity curves (TACs). Although PET imaging has many advantages, there are still some issue for improvement in terms of estimation quality from the time activity curves obtained from PET. TACs enable to estimate kinetic parameters of the compartment models, which give important information about the physiology. Dynamic PET yields low ratios of signal to noise (SNR) and that causes low precision in estimated kinetic parameters. The low SNR results in large spatial variance of parametric images formed by highly

varying kinetic parameters estimated for each pixel. Several studies that concentrate on TAC denoising and population based constraints in order to reduce this variation.

Kinetic modeling is the process of applying mathematical models to analyze the temporal tracer activity, in order to extract clinically or experimentally related information. In region of interest (ROI) analysis, the kinetic parameters are estimated for a region whose pixels have similar kinetic parameters. Therefore, SNR and the precision of estimated kinetic parameters are increased by taking the average of TACs obtained from the pixels within a region. In other methods, TAC are denoised using spatial and/or temporal information. The dynamic PET data was transformed in order to get image reconstructions with high SNR in Hong's paper [2]. Saad et al. got rid of the spatial variance in the kinetic parameters by using TAC region segmentation and parameter estimation at the same time [3]. Qi and Huessman eliminated noise of TAC in the ROI by applying spatial regularization in the reconstructed emission images [4]. Fessler and Rogers [5] proposed an alternative approach that analyzes the mean, variance, and spatial resolution at a fixed point of the objective function.

Many factors affect the precision and accuracy of the estimated kinetic parameters and were studied in the past, such as kinetic models [6], model-fitting algorithms [7]. Wang and Qi extended this work to dynamic PET quantification [8].

Spatial regularization on the kinetic parameter domain is another method that is overlooked in the literature so far. Kamasak et all investigated effects of a quadratic spatial regularization in terms of bias and variance [9]. The effects of spatial regularization on the parametric images might offer an alternative solution. The purpose of the thesis is to investigate the effects of the spatial regularization at various signals to noise levels.

The primary focus was the effects of spatial regularization on kinetic parameter estimations for dynamic PET. For this objective, bias and variance are investigated using a simulated dataset at different noise and spatial regularization levels. The results on simulated parametric image show that the effects of spatial regularization on variance depend on the size of the region and the amount of difference in parameter values in the neighbouring regions. Hence, spatial regularization should be used carefully, especially if the region of interest is small in size and has a large

difference in kinetic parameter value with its surrounding regions. In addition, the effects of noise level on variance of estimated kinetic parameters decrease with the increasing level of spatial regularization.

This thesis is organized as follows; section 1.1 gives brief information about the positron emission tomography and section 1.2 introduces the two tissue compartment model and section 1.3 briefly describes kinetic parameter estimation with different spatial regularization parameters. Section 2 presents methods and the simulation results are given in section 3. Discussion follows the results. Section 5 presents the conclusion.

1.1 Pozitron Emission Tomography

"Molecular imaging" is considered as the main paradigm for twenty-first century biology. Positron emission tomography (PET) is a functional imaging technique that measures local concentration of a radioactive tracer inside the body, widely accepted as a tool for molecular imaging. PET imaging methods were developed in 1970s by a number of researchers including Phelps, Robertson, Ter-Pogossian, and Brownell [10].

In a PET study, a small amount of a detectable positron emitting substance is injected in to the body. This positron labeled tracer is chosen accordingly to follow a certain physiological or biochemical process under study including glucose metabolism, blood, etc. In the process of being labeled with positrons, the tracer becomes a radioactive isotope. The basic idea behind PET is the measurement of the stabilization of a radioactive isotope through the process of positron emission. The decay of the isotope produces a positron, which rapidly undergoes a unique interaction: the positron (e+) combines with an electron (e-) from the surrounding tissue. PET imaging is based on the simultaneous detection of two 511 keV energy photons traveling in the opposite direction. Figure 1.1 shows a schematic diagram of a PET imaging system. It is typical to store and display the raw data from a PET detector ring. In this format, the lines of response are sorted into parallel subsets, each of which represents a projection angle. Each subset (or angle) is represented by a row in an image. The coincidence detection method provides a more sensitive and accurate count of the photon - emission events. In addition, resolution of PET images does not depend on the distance between the emission source and detector. The

image reconstruction process starts with raw data and produces cross-sectional images that represent that radioactivity distribution.

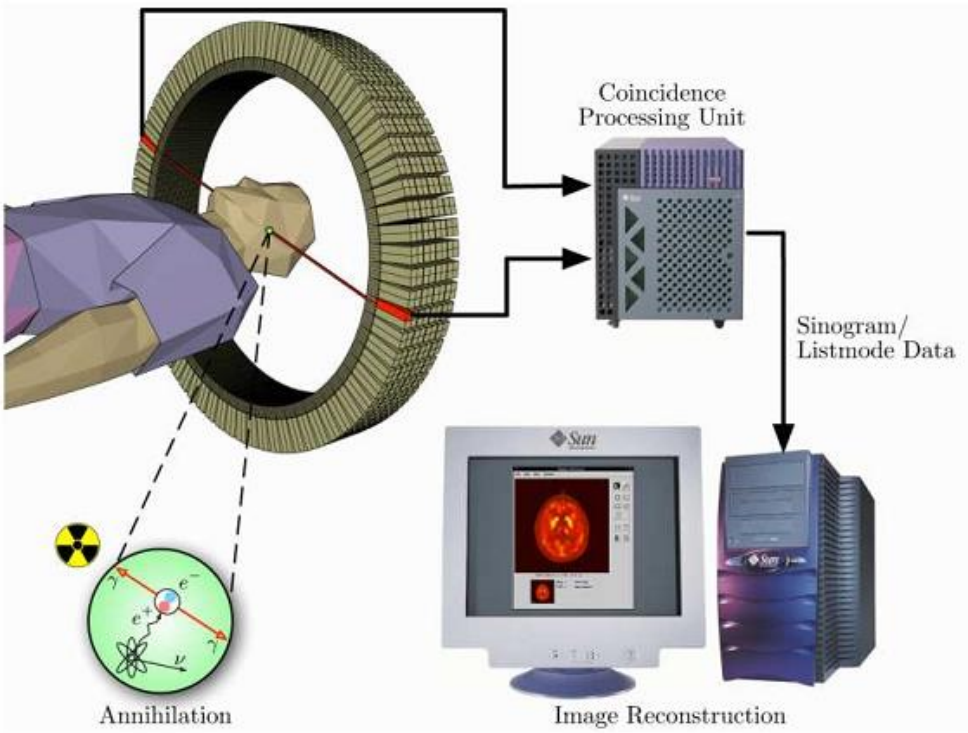

Figure 1.1: PET Imaging Sytems [29]

In PET method, positrons are positively charged electrons, and are emitted by some radioactive isotopes. These radioisotopes are incorporated into metabolically relevant compounds such as raclopride (with ^{11}C), ^{18}F-fluorodeoxyglucose (FDG) and ^{13}N-labelled ammonia. ^{11}C is a widely used PET tracer for measurement of D2 dopamine receptor binding characteristics. The unique interaction of the positron with the matter of the tissue ensures the ability of PET to extract metabolic and functional information of the tissue what constitutes its main advantage. This metabolism information was found to be crucial in conceiving the heterogeneity and invasiveness of tumors. Fallyride is another tracer. It is used PET radioligands for imaging dopamine receptor. The glucose FDG is an example to the most common tracers and FDG images obtained through PET imaging show very significant information about the glucose metabolism and blood flow of the tissue. Their combined usage provides great success in tumor detection and cancer staging. For Alzheimer's studies, FDG is used to measure glucose uptake [11]. Another interesting application of PET is in dynamic cardiac imaging. As an example,^{13}N-labelled ammonia ($^{13}NH3$) can be used

for the measurement of myocardial blood flow which makes it possible to measure blood flow at the level of micro-circulation.

The time dependence of the radioactive decay of a radionuclide is typically expressed with its half-life. The half-life is the time during which radioactivity of the substance is halved. Such a parameterization is appropriate for an exponentially decaying process. Table 1.1 shows some commonly used positron emitting radionuclides and their half - life duration.

Table 1.1: Pozitron Emitter Radionuclides and Their Clinical Uses

Positron Emitting Radionuclides	Two-photon energy(keV)	Half-Life Time(min)	Clinical Use
Fluorine (^{18}F)	511	109	Oncology
Oxygen (^{15}O)	511	2	Myocardial Blood Flow
Nitrogen (^{13}N)	511	10	Myocardial Blood Flow
Carbon (^{11}C)	511	20	Dopamine Receptor Binding

The most substantial benefit of PET imaging is the ability to label very specific biochemical activity and trace it with respect to time. PET imaging is an effective radiological imaging tool in metabolic, blood-flow, functional, and neuroreceptor imaging. In dynamic PET imaging, a series of images are reconstructed obtained by Gamma coincidence detectors. Rahmimet al. gave to dynamic PET imaging consists of independently reconstructing tomographic data obtained within each dynamic frame [12]. Nonetheless, a recent work has denoted that detection time for each event is registered for modern PET scanner capable of collecting the state of a list-mode can be used to further improve the temporal resolution. This is because conventional dynamic PET reconstruction methods assume the activity to be constant within each frame [13]. As a replacement, new approaches make use of temporal basis functions to give the activity in each voxel to be represented continuously over time [14].

In parametric image each voxel represents a value of some physiological parameter, for example perfusion or receptor binding potential, while the original PET image contains radioactivity concentrations. When traditionally modelling is done using regional time activity information, a parametric image is created so that the modelling is performed separately in each voxel. Various approaches to determine the dynamic PET images have been proposed for various functional regions. Barber

extracted the principal components of a Gamma camera dynamic study followed by factor analysis to identify the fundamental functional changes [15]. Recently, Kamasak et al. simultaneously clustered and estimated each cluster's TAC directly from the projection (sinogram) data, without the need for tomographic reconstruction [16].

1.2 Compartmental Models

Compartmental model is an elementary concept to analyze PET data and as compared to distributed models, compartment models have been accepted to be satisfying for describing dynamic PET data. The basis is to model the interaction of the tracer which is a chemical material inside different organs of the human body. The model is constructed on the principle that the compartments will represent various physical locations such as plasma or tissue and the chemical states (i.e. free or metabolized). In addition, there are connections between these compartments that represent the exchange rate of tracer between the compartments in the model. These coefficients are the parameters of the compartment model, and these parameters are generally referred as kinetic parameters [17]. In other words, the flow of tracer among the compartments are formulated by equations and the coefficients of these equations are the kinetic parameters. Compartmental models are described mathematically by a series of ordinary differential equations (ODEs). The equations that are used to formulate the dynamics of tracer are the first order differential equations. The TACs that are extracted from the reconstructed emission images, as explained previously, will be used to estimate the kinetic parameters.

In PET, the volume of the compartment might correspond to the volume of the voxel or to a larger region of interest (ROI). One important application of PET is to quantify the absolute tracer uptake in regions of interest. ROI quantification is very important for evaluating tumor activity, growth rate, and efficacy of therapeutic interventions. Compartments typically correspond to distinct kinetic states taken on by the radiolabeled tracer. Usually, the tracer is introduced into the organism via bolus injection(s) and so the uptake, retention, and eventual efflux of tracer from the tissue region of interest are transient phenomena that never reach steady states. That is, the concentrations of tracer in tissue or plasma do not achieve a constant level. If

the system (tracer and tissues of interest) were to reach equilibrium, the system of ODEs would reduce to a set of algebraic equations that could be solved analytically.

There are many compartmental models and many methods to analyze dynamic PET data. The choice of a specific model configuration is governed by various factors. First, it depends on the properties of the tracer. If the tracer is inert and does not interact with any receptor system or does not undergo any chemical change, but simply diffuses into and back out of the cells, a one tissue compartment model (k_3=k_4=0) would be an appropriate model. Another aspect of a radiotracer is its retention in the target tissue. Tracers like [^{11}C] FMZ are not permanently trapped in the bound state and may convert back to the non-specific state (k_4>0). However, a tracer like [^{11}C] N-methylpeperine propionate ([^{11}C] PMP) is metabolized by the enzyme acetocholinesterase (AChE) and the metabolized state is retained in the tissue (k_4=0) [18]. Thus, the reversibility of a tracer must be considered prior to choosing the model configuration.

The simplest compartment model is called one-tissue compartment. In one-tissue compartment model, there is only one compartment in tissue and exchange radiotracer between plasma compartment (C_p) and tissue compartment (C_T) by two rate constants k_1 and k_2. The most common application of the one tissue compartment is blood flow measurement by ^{15}O labeled water. The one tissue compartmental model is sometimes enough for many radioligands to describe their kinetics. One tissue compartment model is shown in Figure 1.2. The tracer dynamics of one tissue compartment model can be described as:

$$\frac{d}{dt}C_T(t) = k_1 C_P(t) - k_2 C_T(t) \qquad \textbf{(1.1)}$$

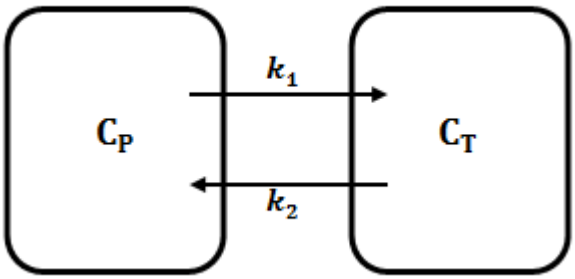

Figure 1.2 : One Tissue Compartmental Model

Biologically accurate models may not be practical. A model with higher complexity may be more accurate biologically, but may have too many parameters, and hence it would be impossible to estimate accurately all of the model parameters. Some models might work when statistical noise is low, but yield multiple solutions for high noise cases. Thus, model simplification may be required and some bias in parameter estimates will need to be allowed in order to obtain better precision. A number of configurations might have to be tested before choosing an appropriate model. For [^{11}C] raclopride, a two-tissue compartment model has been shown to be a satisfactory model [19].

Figure 1.3 shows two compartments model and this model consists of three compartments. First compartment is the plasma compartment (C_P) represents the tracer concentration in the plasma. C_P is measured by sampling blood from the patient during the scan. The other compartment is called C_{T1}, the free compartment, represents tracer concentration in the tissue that is not metabolized or bound. The last compartment is named C_{T2}, the bound compartment, represents tracer concentration in the tissue that is metabolized or bound. The model depends on the kinetic parameters, k_1, k_2, k_3, and k_4, which specify the tracer exchange rates between compartments in units of inverse minutes. The two tissue compartmental model fits many radioligand tracers such as FDG, ^{11}C-raclopride and ^{18}F-fallypride well. Therefore, this model can be used for tracers that have two distinct chemical states within the tissue. Each compartment describes a different state of the tracer molecule inside the body. ^{11}C-raclopride is a typical example of the two tissue compartmental model and this tracer is also commonly used to determine the activity of dopaminergic drugs. Another example, in brain PET imaging, the tracer molecule is injected through the blood and then binds to brain receptors specific to this tracer, or metabolizes inside the tissue. Once tracer paths between compartments are specified, the mass balances between compartments are modelled using a set of ordinary differential equations (ODEs).

The ODEs for two tissue compartmental model are given by

$$\frac{d}{dt}C_{T1}(t) = k_1 C_P(t) - (k_2 + k_3)C_{\mathrm{T1}}(t) + k_4 C_{\mathrm{T2}}(t) \quad \textbf{(1.2)}$$

$$\frac{d}{dt}C_{T2}(t) = k_3 C_{T1}(t) - k_4 C_{\mathrm{T2}}(t) \quad \textbf{(1.3)}$$

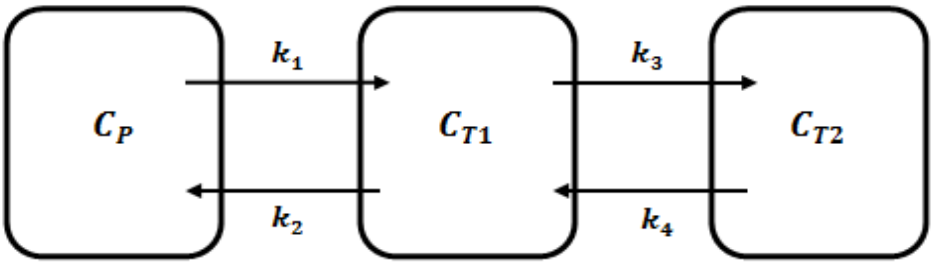

Figure 1.3 : Two Tissue Compartmental Model

Solving the ODE's in Equation **(1.2)** and Equation **(1.3)**, the following equations can be written:

$$C_{\mathrm{T1}}(t) = \left\{\frac{k_1}{\alpha_2 - \alpha_1}[(k_4 - \alpha_1)e^{-\alpha_1 t} + (\alpha_2 - k_4)e^{-\alpha_2 t}y(t)\right\} * C_P(t) \quad \textbf{(1.4)}$$

$$C_{\mathrm{T2}}(t) = \left\{\frac{k_1 k_3}{\alpha_2 - \alpha_1}[e^{-\alpha_1 t} - e^{-\alpha_2 t}]u(t)\right\} * C_P(t) \quad \textbf{(1.5)}$$

where $*$ indicates convolution,

$$\alpha_1, \alpha_2 = \frac{(k_2 + k_3 + k_4) \mp \sqrt{(k_2 + k_3 + k_4)^2 - 4k_2 k_4}}{2} \quad \textbf{(1.6)}$$

where roots are assumed to be real constants, a reasonable assumption in modeling based on standard physiological values for k_2, k_3 and k_4.

We transform the kinetic parameters (k_1, k_2, k_3 and k_4) to new parameter (a, b, c, d) that are well suited for optimization. However, kinetic parameters are more physiologically related.

1.3 Kinetic Parameter Estimation With Spatial Regularization

Kinetic modeling (KM) is an important tool in Positron Emission Tomography which enables us to study the kinetics of tracers. It is the process of applying mathematical models to analyze the temporal tracer activity. The rate of exchange of tracer between compartments is given by a rate constant k (in fraction per time, min^{-1}).

Kinetic parameters of tissue perfusion, tracer transport or receptor binding are calculated by fitting the average time activity curves within a region of interest to underlying mathematical models. Generally, the kinetic modeling process begins by marking a region of interest around different functional regions. The PET activity is then averaged over the ROI at each time frame, and a single set of kinetic parameters

is estimated by fitting a single kinetic model to the time sequence of average activities. ROI quantification is very important for evaluating tumor activity, growth rate, and efficacy of therapeutic interventions. Manual ROI description of functional regions is a tedious, time-consuming, and error-prone. This leads to inaccuracies in kinetic parameter estimation.

The kinetic modeling is performed based on the average TAC for each region. TAC gives useful information about the kinetics of the radiotracer in the specific tissue and at the same time gives insight about the rate of tracer in and out flux and amount and rate of tracer accumulation. The activity images is formed into various time frames and reconstructed to obtain PET image data which represents the radiotracer distribution in tissue at specific time points. The effects of the spatial regularization on the estimation of kinetic model parameters are studied for each voxel corresponding to a PET image. The results are available to analyse the effects of regularization quantitatively.

Carson and Lange [20] proposed direct estimation of kinetic parameters from PET data in 1985. They outlined a general framework for a direct reconstruction algorithm based on expectation-maximization iterations. The accuracy and reliability of the estimated kinetic parameters are very crucial. Fessler et al investigated effect of spatial regularization on bias and variance [21]. Qi and Huessman proposed the use of ROI analysis of emission tomography (PET and SPECT) [22]. To simplify practical implementation, Wang and Qi et al proposed generalized optimization transfer algorithms for direct penalized likelihood reconstruction of parametric images that are applicable to a wide variety of kinetic models [23]. In 2005, a parametric iterative coordinate descent (PICD) algorithm was proposed by Kamasak for penalized likelihood estimation of parametric images of a two-tissue compartment model [24]. The total measured activity concentration of the PET from plasma and tissue compartments as a function of time is given by

$$C_{total}(t) = f_v C_P(t) + (1 - f_v)\{\sum_{i=1}^{N} C_{Ti}(t)\} S_A e^{-\lambda t} \qquad \textbf{(1.7)}$$

In this equation f_v indicates the fraction of plasma within the tissue, S_A shows the initial specific activity of the tracer (ie efficiency of radioactive labeling, nCi/pmol), and λ indicates the decay constant for the radioactive isotope (min^{-1}). N is the number of compartments in the study.

The model based TAC can be enumerated at discrete times by averaging the measurements for any voxel k from Equation **(1.7)**. Let the parameters of compartment model be listed in vector form as using $\theta = [k_1, k_2 \dots, k_p]$ $(\theta \epsilon \mathbb{R}^p)^1$. In addition, let $f(\theta, t)$ indicate the forward model that models C_{total}(t) with given θ and t.

Let X= $[x_1 x_2, \dots., x_k]$ denote the vector of TAC measurements that are taken at K discrete time at t=$(t_1 t_2, \dots., t_K)$ .This equation is given by

$$x_k = \frac{1}{t_k+1-t_k} \int_{t_k}^{t_k+1} C_{total}(t)dt \qquad \textbf{(1.8)}$$

The parameter vector for voxels can be estimated by minimizing the weighted squared error difference between the measured time activity curve (x) and the model predicted curve $f(\theta, t) = |f(\theta, t_1), f(\theta, t_2), \dots, f(\theta, t_K)|$ as follows:

$$\widehat{\theta} = arg \min_{\theta \geq 0} \|x - f(\theta, t)\|_W^2 \qquad \textbf{(1.9)}$$

where, W is the weighting matrix that takes into account the difference in variance between different frames of the PET scan , $\hat{\theta}$ is the estimated kinetic parameter. In spite of the fact that there are many different way to choose the weights, the most commonly used weights are given by

$$W = diag\left\{\sqrt{\frac{\Delta t_k}{\mathcal{X}_k}}\right\} \qquad \textbf{(1.10)}$$

where $\mathcal{X}_k$ is the measured time activity and Δt_k is the scan duration for time frame k. Kinetic parameters estimated for all pixels form a spatial parametric image, $\Theta = [\theta_1 \theta_2, \dots \theta_N]$, where θ_i denote the kinetic parameters for pixel i, and N denotes the total number of pixels in the parametric image. The primary focus was the effects of spatial regularization on kinetic parameter estimations for dynamic PET.

The spatial variance of the kinetic parameter estimates can be reduced by adding a stabilizing function to equation. The resulting estimate is given by

$$\widehat{\Theta} = arg \min_{\Theta \geq 0} \|X - f(\Theta)\|_W^2 + \beta R(\Theta) \qquad \textbf{(1.11)}$$

In this equation, time activitiy curve values is X = $[\mathcal{X}_1 \mathcal{X}_2, \dots, \mathcal{X}_N]$ for all pixels, $R(\Theta)$ denotes the penalty term and β denotes a constant that adjusts the amount of regularization.

If the kinetic parameters for each pixel is estimated independently, the resulting parametric image typically will have very high spatial variance resulting from low SNR of the dynamic PET data. Therefore, the spatial variance of the parametric images is needed to be investigated. The regularization parameter adjusts the spatial smoothness of the parametric image. High regularization parameter increases the contribution of the image model to the cost function given in Equation **(1.9)**. This equation an extra regularization term is added to penalize the local changes in the parameter values. This method is named kinetic parameter estimation with spatial regularization. When $\beta = 0$, this will be equivalent to the independent estimation case described above, and when $\beta = \infty$ a flat parametric image will be obtained. Therefore, a trade-off can be made between bias and variance by adjusting β parameter.

We investigate the effects of a spatial regularization term is given by

$$R(\Theta) = \sum_s \sum_r g_{sr}\, \psi(\theta_s, \theta_r) \qquad \textbf{(1.12)}$$

where θ_s shows the kinetic parameters at pixel s, θ_r shows the kinetic parameters at pixel r. g_{sr} indicates the penalty weight for the difference in the kinetic parameters of pixel s and r, and $\psi(\theta_s, \theta_r)$ indicates the the amount of penalty.

For punishing local changes, the following equation is used.

$$g_{sr} = \begin{cases} 1, & If\{s,r\}\epsilon N \\ 0, & Otherwise \end{cases} \qquad \textbf{(1.13)}$$

where N shows the set of neighbouring pixel pairs. For ψ, there are many M-estimators such as L_2 norm, Huber norm, L_1 norm, Cauchy, Tukey and so on. L_1 regression minimizes the sum of the absolute errors while L_2, another name for ordinary least squares, minimizes squared errors. Consequently, L_1 gives much less weight to large deviations. The functions ψ for L_1, L_2 and huber are shown in Figure 1.4.

We choose the L_2 norm:

$$\psi(\theta_s, \theta_r) = \|\theta_s - \theta_r\|_{\prod}^2 \qquad \textbf{(1.14)}$$

where $\prod$ indicates a diagonal matrix that weights the changes in the kinetic parameters. L_2 norm is not robust because its influence function is not bounded.

Therefore, the kinetic parameters do not make good estimation for edges of dynamic PET imaging.

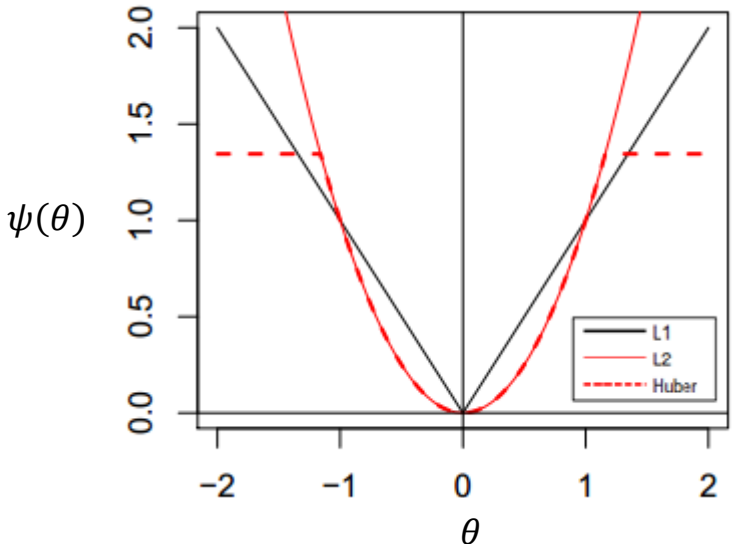

Figure 1.4: M-Estimators

2. METHOD

In this section, first we describe about the phantom image and dataset, then describe the test method.

First of all, an image is cretated with two different regions other than background by using MATLAB and Figure 2.1 shows the phantom image. Phantom has resolution of 128×128. Phantom image has three regions including the background. The background region (BG) is a square region, and two foreground regions are circles with different radius which are both our region of interest (ROI). ROI 1 stands for region of interest with large radius whereas ROI 2 stands for region of interest with small radius in this thesis. The TAC of a ROI is then extracted from the images and is used to estimate tracer kinetic parameters based on a compartmental model. Kinetic modeling parameters of tissue perfusion, tracer transport or receptor binding are typically calculated by fitting the average time activity curves within a region of interest to underlying mathematical models. In this thesis, we focus on ROI and kinetic modeling parameter estimation from dynamic PET imaging.

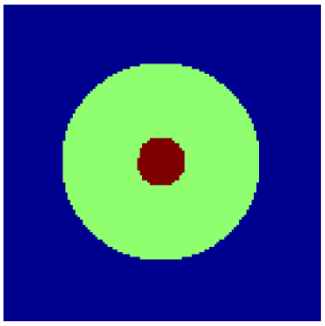

Figure 2.1: Phantom Image

Table 2.1 shows the dataset which gives the kinetic parameter values for two different foreground regions. The kinetic parameters are taken from Kamasak et al [9]. The kinetic parameters (k_1, k_2, k_3, k_4) represent the rates of exchange of the raclopride between the compartments. Using these kinetic parameters, phantom images are created and simulations are performed by using set of kinetic parameters.

The aim of a PET study is the estimation of these rate parameters which contain the important quantifiable pharmacological information of the system.

Table 2.1: Kinetic Parameter Values in simulations

Region	k_1	k_2	k_3	k_4
ROI 1	0.1860	0.8968	0	0
ROI 2	0.0918	0.4484	1.2408	0.1363

Figure frame shows the radiotracer distribution in phantom image from a 60 min [^{11}C] Raclopride PET study. The data collected was divided into 18 frames of different time durations (from 0.5 min to 5 min) and each time frame was reconstructed to yield an average radioactivity distribution image for that frame is shown in Figure 2.2.

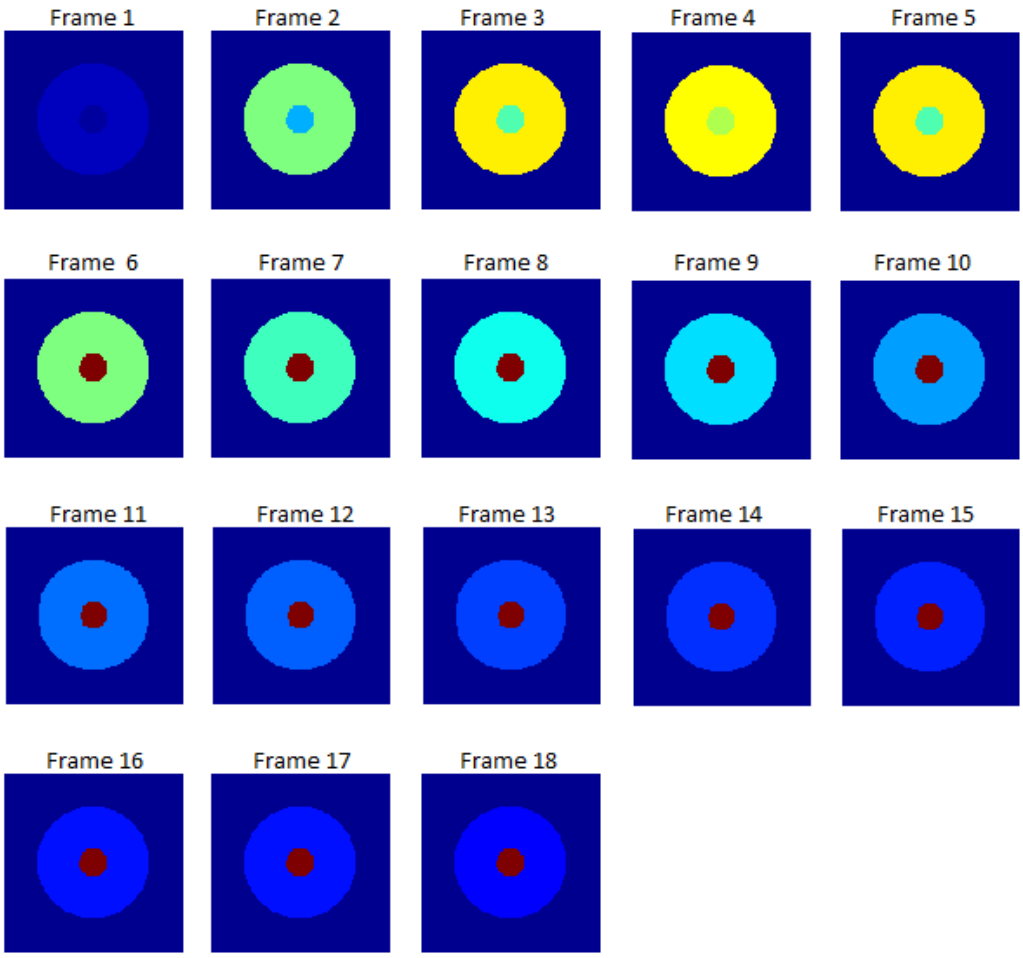

Figure 2.2: Dynamic sequence of a slice of a phantom image

Tracer concentration in individual voxels or regions changes within the time of the image is called a time activity curve. These TACs are useful in quantifying the

physiological (e.g. blood flow) and/or pharmacological aspect (e.g. receptor binding site density, enzyme activity) of the system of interest. A sequence of dynamic images that represent the tracer distribution over time is reconstructed. Time activity curves for two foreground regions of noiseless PET image activities from the study in above figure are shown in Figure 2.3.

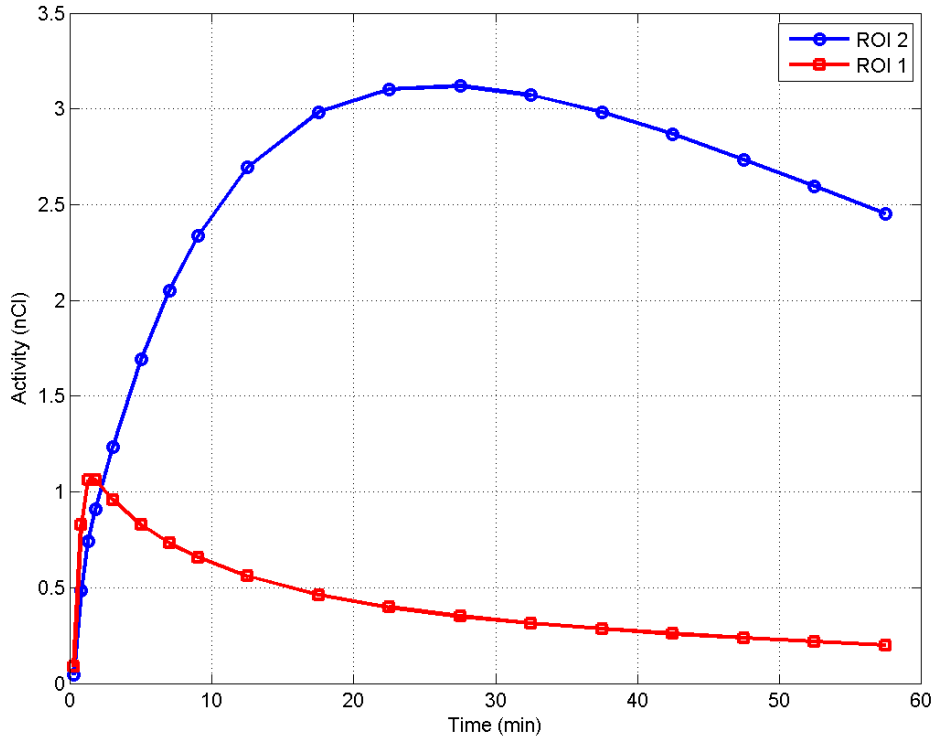

Figure 2.3: Noiseless TAC for two different foreground regions

Raclopride which includes 11C is used as a tracer and its decay constant is $\lambda = 0.034$ min^{-1}. The primary assumption is that the blood contribution to the PET activity (fv) is zero. Time frames of PET image are generated using the phantom and the two-tissue compartment model equations. Total scan time is 60 minute that are divided into 18 time frames of different time durations. Each of the first four time frames are observed 0.5 minutes duration due to the fact that tracer initially diffuses significantly fast. The next four frames are measured 2 minutes duration. Each last ten frames are observed 5 minutes duration because tracer diffusion does not change rapidly.

PET images generally have low signal to noise ratio and time activity curve extracted from a single pixel may be very noisy. However, exact modeling of the noise distribution of PET images can be difficult since noise is spatially variant and object-

dependent. Usually the spatial variation and correlations between pixels are simply ignored in the kinetic fitting step, which can lead to very noisy results. Therefore, each phantom image is generated at six different levels with 0.5 dB, 1 dB, 4 dB, 8 dB, 10 dB and 20 dB signal to noise ratio by using additive white gaussian noise (AWGN) function of MATLAB. Parametric images are estimated after four different types of spatial regularization which are no spatial regularization (NR), low spatial regularization (LR), medium spatial regularization (MR) and high spatial regularization (HR).

3. RESULT

In order to evaluate the performance of our algorithm, we simulated parametric images with four different spatial regularization parameters. This work proposes a solution for different noise values according to the effects of spatial regularization on parametric images. Simulations are run by using four different spatial regularization methods as no, low, medium and high spatial regularization. Analysis of parametric images shows that proper selection of the regularization parameters is important for dynamic PET. After experimental work, the best regularization parameter for each spatial regularization type is found. Therefore, it is concluded that the choice of the regularization parameter has a significant impact on the kinetic parameter estimation, indicating proper selection of image parameters is important for dynamic PET quantification. Parametric images are obtained by estimating the kinetic parameters of each pixel by applying different amount of spatial regularization.

Simulation experiments are based on phantom images. Kinetic parameters for the regions which applied to the phantom images are taken from Kamasak et al [9]. Using the frame 12 of the phantom image, noisy images are shown at different noise levels which are given in Figure 3.1. The SNR values for these noisy images are 0.5 dB, 1 dB, 4 dB, 8 dB, 10 dB and 20 dB, respectively.

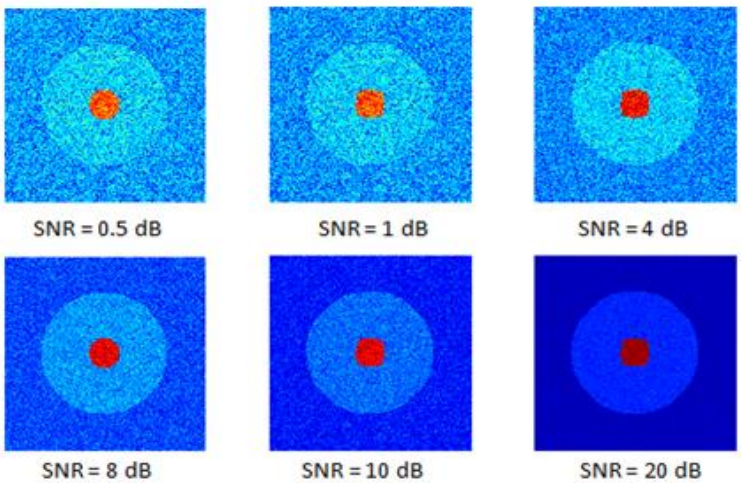

Figure 3.1: Noisy images of time frame 12 of dataset at different SNR values

The kinetic parameters were estimated and parametric images were produced using no spatial regularization (NR), low spatial regularization (LR), medium spatial regularization (MR), and high spatial regularization (HR). 10^2, 10^3 and 2×10^4 were selected as the regularization parameter (β) values in Equation **(1.11)** for LR, MR, and HR, respectively. Moreover, the Π matrix that denotes a diagonal matrix that weights the changes in kinetic parameters was taken as $\mathrm{diag}\left\{\frac{1}{3},\frac{1}{65},\frac{1}{56},1\right\}$for Raclopride.

We show some simulation results to demonstrate effects of spatial regularization with different noise levels. We simulated a 60 minute raclopride using a phantom that consist of two regions. The time activity curve of each region was generated using a two-tissue compartment model and an analytical blood input function.

Figure 3.2-3.7 show the parametric images that are estimated from the kinetic parameters obtained using different types of spatial regularization for 0.5 dB, 1 dB, 4 dB, 8 dB, 10 dB and 20 dB SNR values, respectively. Low regularization parameter deemphasizes the image model and assigns the images depending more on the acquired data. This allows the output parametric images to deviate from the image model. The regularization parameter should be chosen depending on the SNR of the data. As the SNR decreases, higher regularization parameter should be chosen to make the results less sensitive to the noise.

Figure 3.2 shows the parametric images which are estimated from the kinetic parameters obtained using different types of spatial regularization for 0.5 dB SNR value. The first row contains the original parametric images. The remaining rows are respectively the reconstructions of NR, LR, MR and HR spatial regularization on the k_1, k_2, k_3 and k_4 parametric images. It can be seen that when the spatial requlariza tion inclines, the information in the edges and other details are lost which causes smoother parametric images. Consequently, this information loss in edges is the reason of the difference between the real values and the parameter values of the foreground regions. We observed that the parametric image processed using the HR was the best estimation for k_1 and k_2 which showed more details even after high levels of noise was added. On the other hand, MR spatial regularization gives better estimation than others for k_3 parametric image. Moreover, k_4 parametric image is estimated with lowest error when LR spatial regularization is applied.

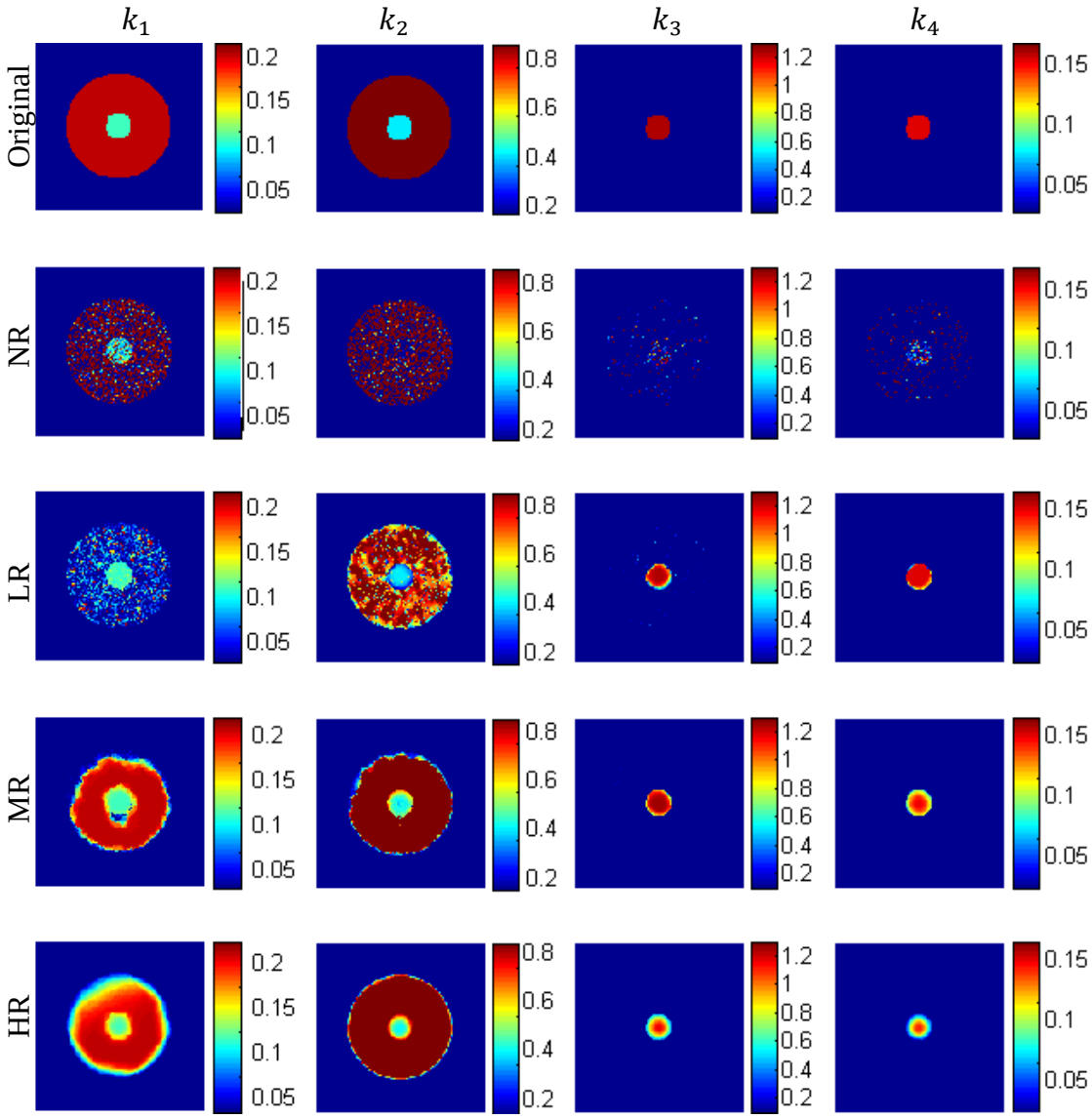

Figure 3.2: Parametric images of k_1, k_2, k_3 and k_4 estimated by NR, LR, MR and HR for 0.5 dB SNR value.

Figure 3.3 shows qualitatively the comparison between the four different spatial regularization algorithms for 1 dB SNR value. As the regularization parameter increases, the parametric images become smoother. It can be clearly seen that the parameter images are totally missing in the NR and LR algorithms, but MR and HR were able to capture them. Therefore, higher regularization parameter should be chosen to make the results less sensitive to the noise. In order to compare between the algorithms quantitatively for the k_1 and k_2 parametric images, it can be clearly seen that MR and HR are better estimation. Moreover, LR spatial regularization gives best estimation for k_3 and k_4 parametric images.

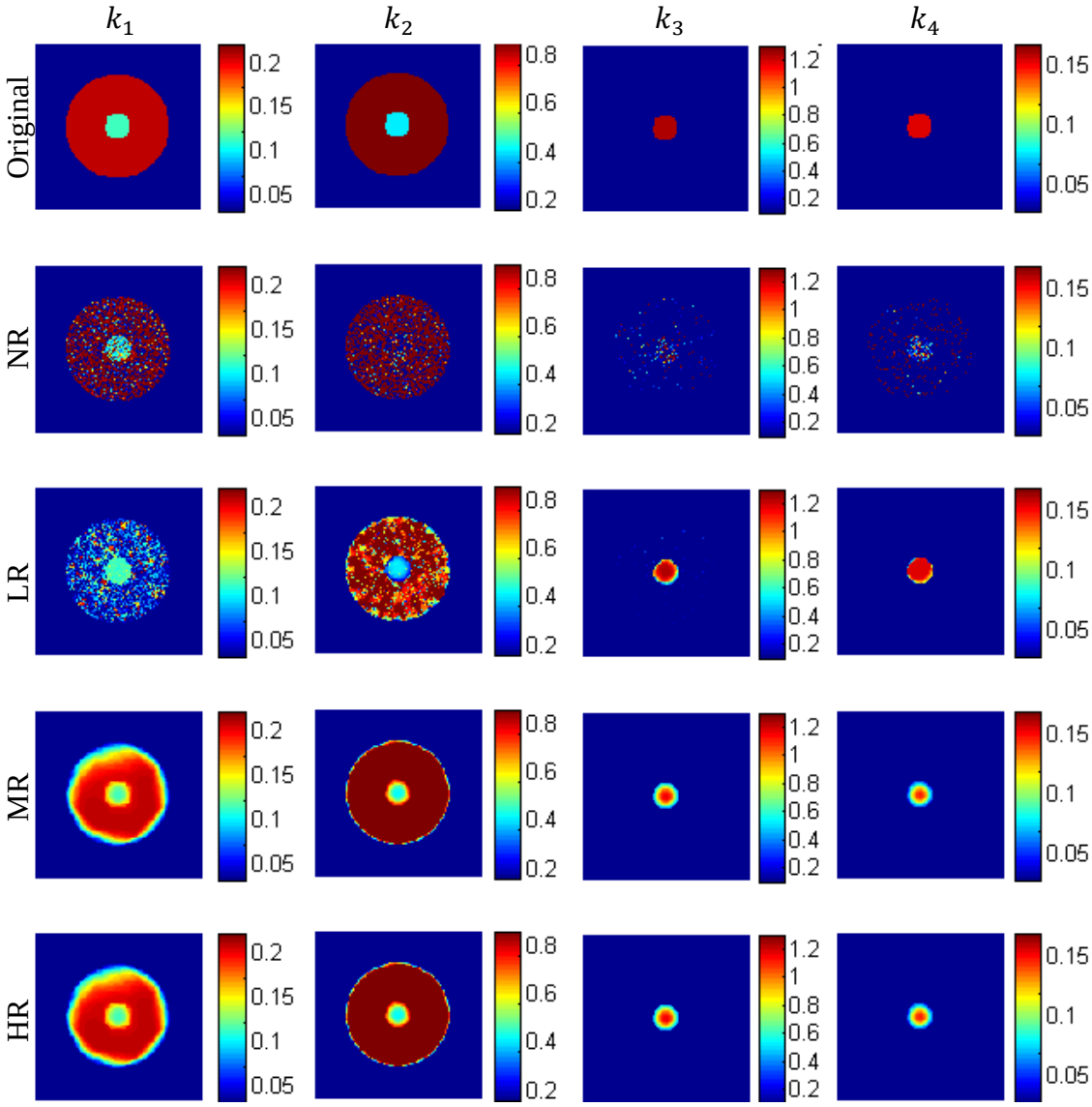

Figure 3.3: Parametric images of k_1, k_2, k_3 and k_4 estimated by NR, LR, MR and HR for 1 dB SNR value.

Various regularizations parameters were applied directly to the k_1, k_2, k_3 and k_4 parametric images for 4 dB SNR value so the results of the algorithm are shown in Figure 3.4. This figure displays the kinetic parameter reconstructions with the original images and with the estimated parametric images. All kinetic parameters in this figure are estimated with different regularizations on k_1, k_2, k_3 and k_4. We observed that the parametric image of k_1 and k_3 processed using the MR were showed more details even after noise was added.

Figure 3.5 shows the parametric images which are estimated from the kinetic parameters obtained using different types of spatial regularization for 8 dB SNR values.

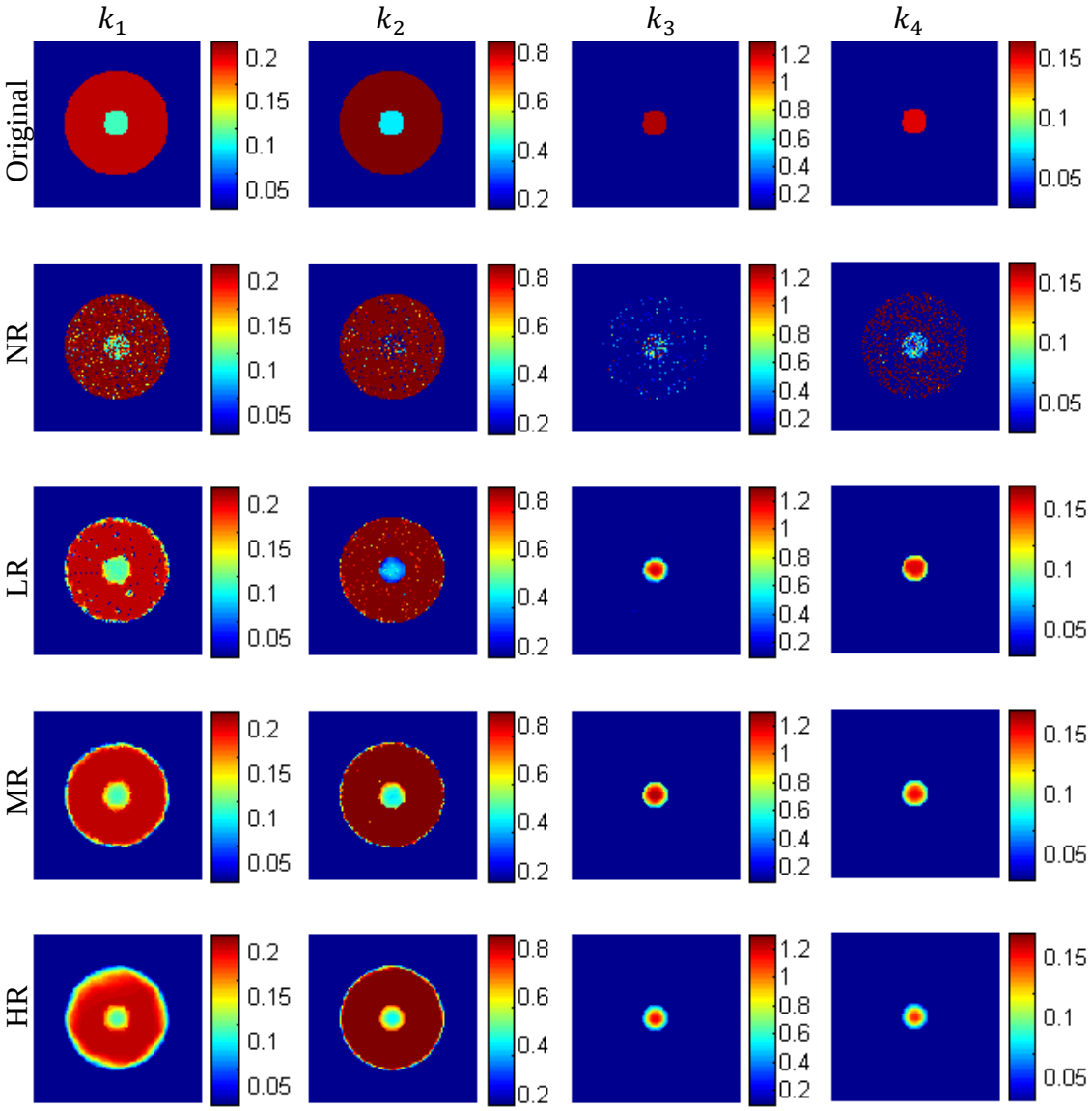

Figure 3.4: Parametric images of k_1, k_2, k_3 and k_4 estimated by NR, LR, MR and HR for 4 dB SNR value.

The parametric images that are estimated from the kinetic parameters obtained using different types of spatial regularization for 10dB are demonstrated in Figure 3.6. We observed that the parametric image of k_2, k_3 and k_4 processed using the MR were best estimation after 10 dB of noise was added.

Figure 3.7 shows the original parametric images and estimated parametric images with various spatial regularization parameters. When the regularization parameter is increased, MSE of parametric images is also increased. Further, we compared the parametric images acquired with k_1 and k_2 processing to ensure preservation of images in LR.

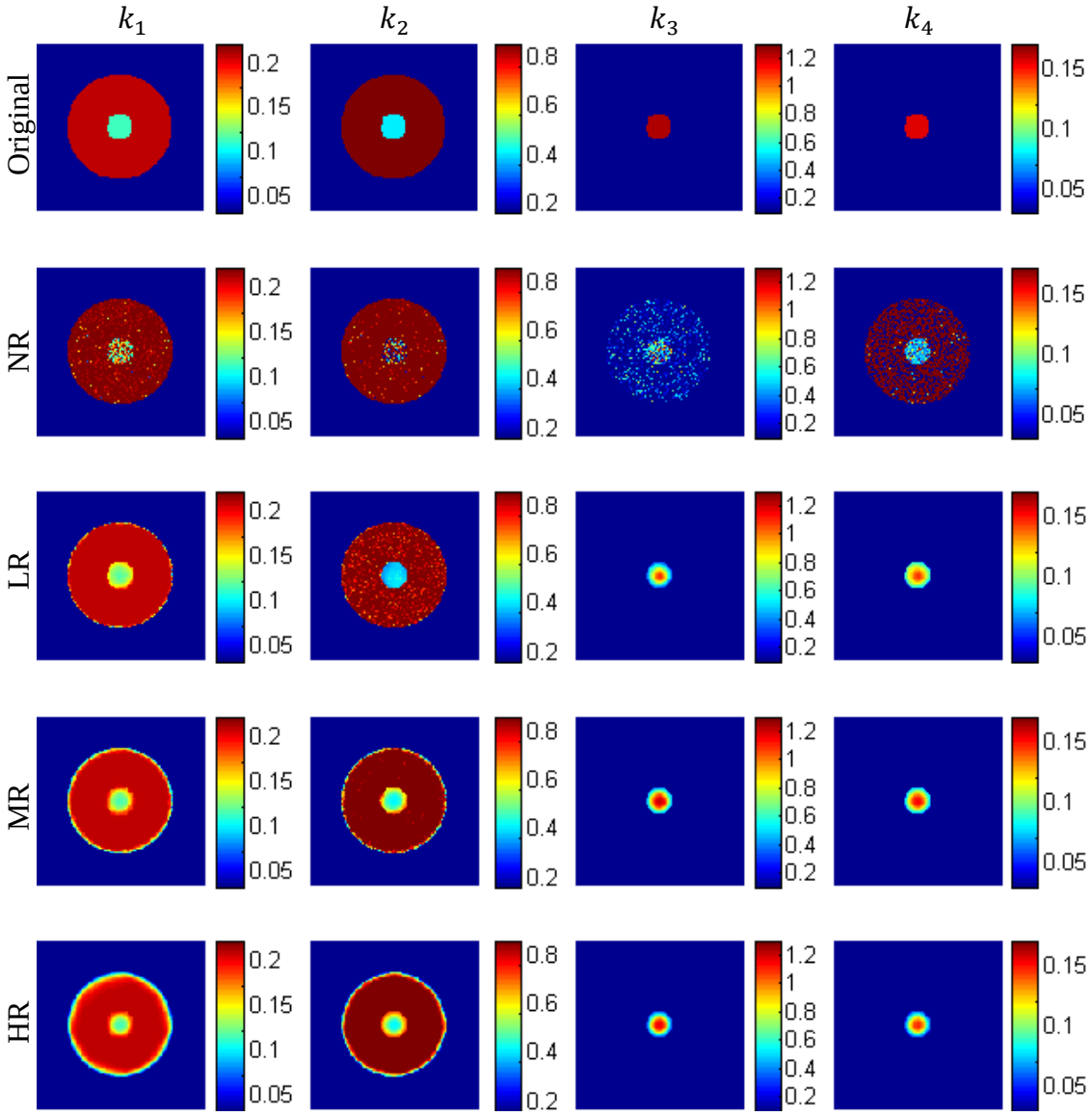

Figure 3.5: Parametric images of k_1, k_2, k_3 and k_4 estimated by NR, LR, MR and HR for 8 dB SNR value.

64th row of 128x128 each parametric image, which has low spatial regularization, medium spatial regularization and high spatial regularization are plotted in the same figure at 0.5 dB SNR value. Parametric images with original, LR, MR and HR are plotted using yellow, blue, cyan and red colors respectively. The result for 0.5 dB SNR value is shown in the Figure 3.8.

It can be shown from the k_1 image that parametric image with high spatial regularization provides the best estimation to the original image. The parametric image with medium spatial regularization gives better estimation than the parametric image with low regularization. From this figure, it can be seen that the parametric images obtained with low regularization have rapid changes. The original image is

estimated better with high spatial regularization for k_2 parametric image. The parametric image with low spatial regularization provides better estimation than the parametric image with medium spatial regularization. It can be shown from the k_3 and k_4 images that parametric images with medium and low spatial regularization provide better estimation than the parametric image with high regularization.

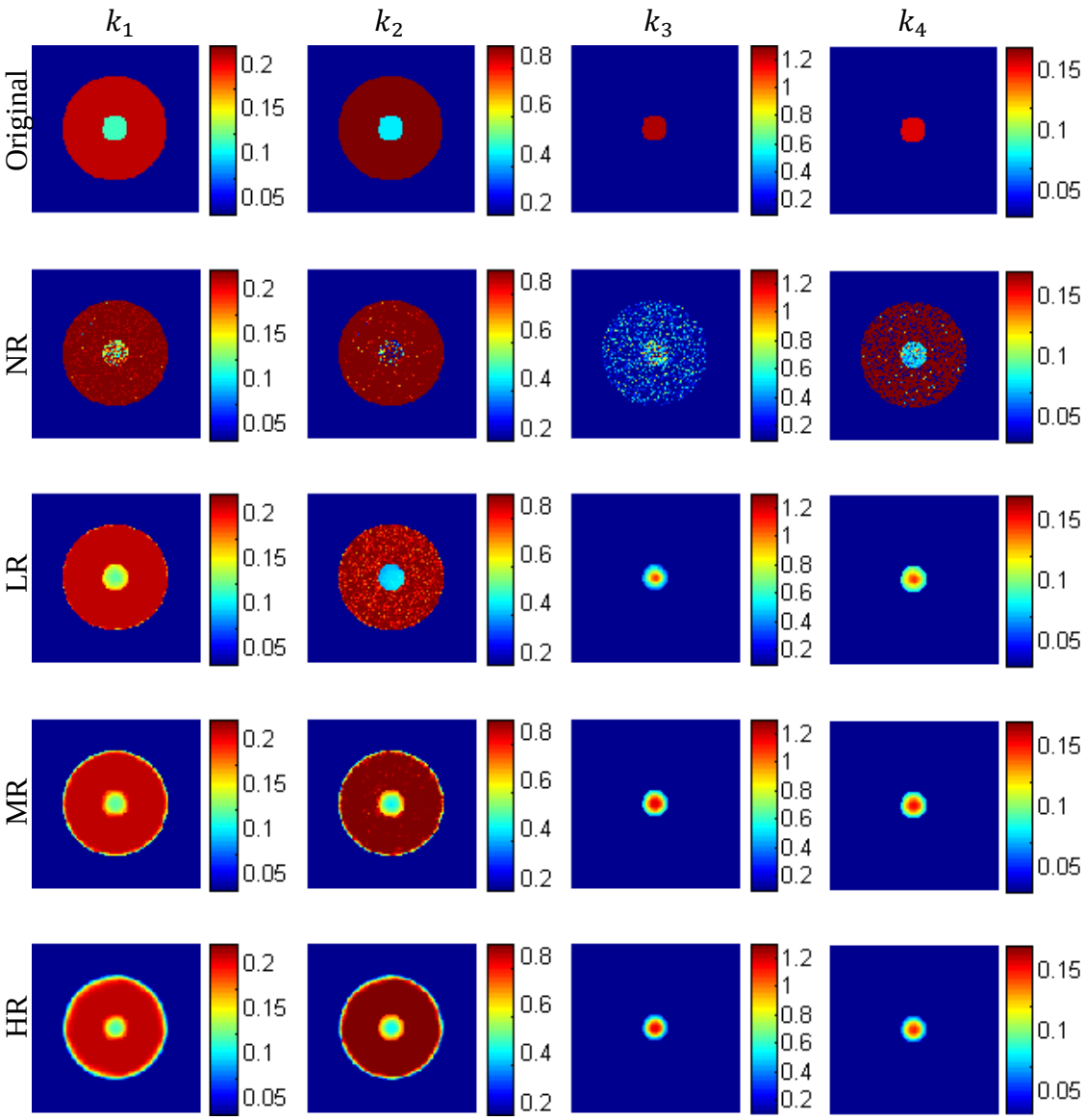

Figure 3.6: Parametric images of k_1, k_2, k_3 and k_4 estimated by NR, LR, MR and HR for 10 dB SNR value.

The same procedure is applied to parametric images with LR, MR, HR at different SNR values. The results for other SNR values are shown in the Figure 3.9-3.13, respectively. The result for 1 dB SNR value is shown in the Figure 3.9.

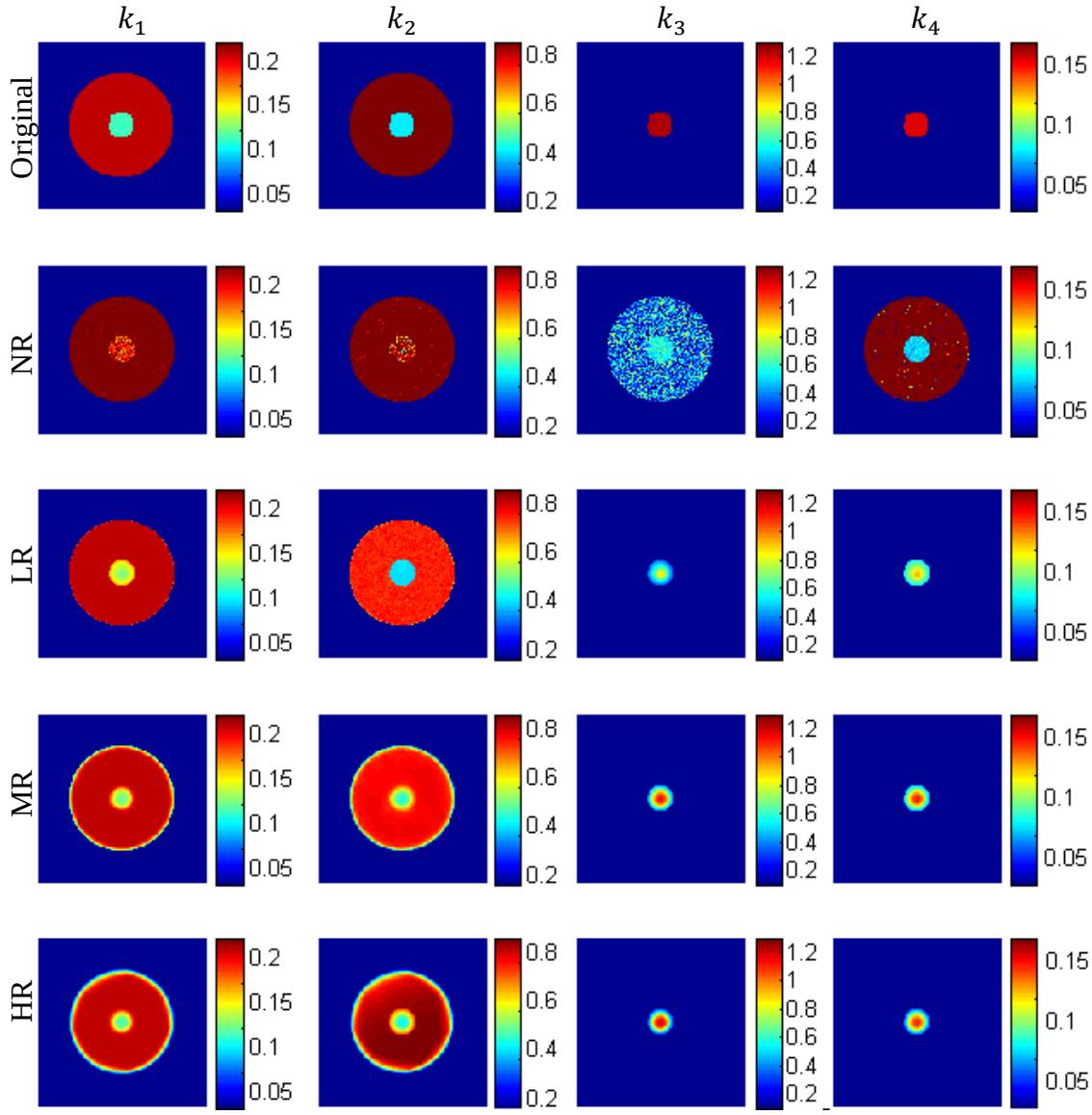

Figure 3.7: Parametric images of k_1, k_2, k_3 and k_4 estimated by NR, LR, MR and HR for 20 dB SNR value.

It can be shown from the k_1 image that parametric image with low spatial regularization cannot converge to the original image due to fluctuation. The parametric images with medium and high spatial regularization give approximately the same estimation to the original image. k_1 and k_2 parametric images with low spatial regularization cannot follow original image. In other words, the parametric image with low spatial regularization provides worse estimation than the parametric images with medium and high spatial regularization. k_3 and k_4 parametric images with low spatial regularization give the best estimation to the original image.

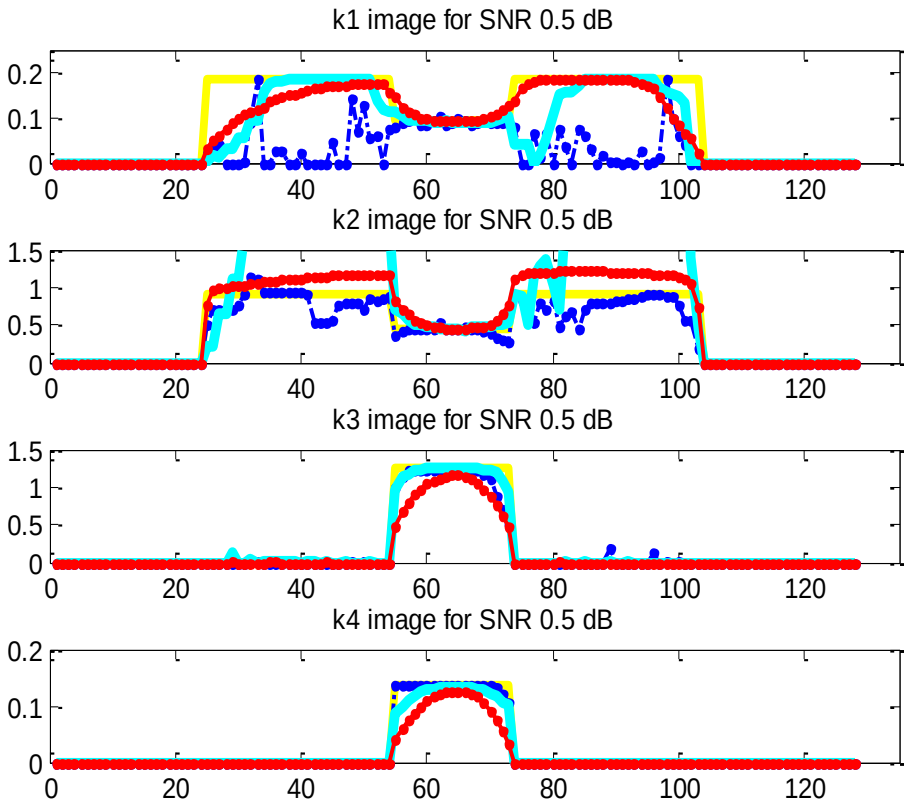

Figure 3.8: Profile of 64th row obtained parametric images with different spatial regularization for 0.5 dB SNR. Parametric images with original, LR, MR and HR are plotted using yellow, blue, cyan and red colors respectively

From k_1 image, the parametric image obtained with low regularization have changes in some value is shown in the Figure 3.10. Therefore, the parametric images with medium and high spatial regularization provides better estimation to the original image than the parametric image with low spatial regularization. k_2 parametric images with medium and low spatial regularization cannot converge to the original image due to fluctuation. The parametric images obtained with high regularization provides approximately the same estimation to the original image. For k_3 and k_4 parametric images, simulation results with different spatial regularization are very close to the original image.

As shown in Figure 3.11 and Figure 3.12, k_1 image reconstructed by using low and medium spatial regularization is approximately similar to original whereas k_2 parametric images with medium and low spatial regularization cannot converge to the original image due to fluctuation. The k_2 parametric images obtained with high regularization give approximately the same estimation to the original image. It can be

shown from the k_3 and k_4 images that parametric images with medium spatial regularization provides better estimation than other spatial regularizations.

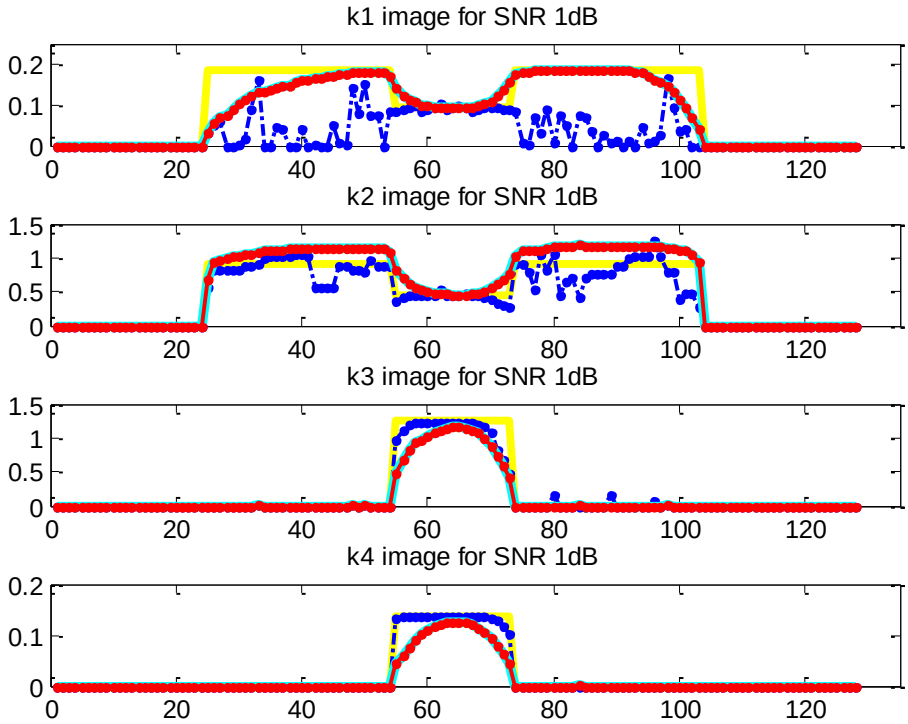

Figure 3.9: Profile of 64th row obtained parametric images with different spatial regularization for 1 dB SNR. Parametric images with original, LR, MR and HR are plotted using yellow, blue, cyan and red colors respectively.

It can be shown in Figure 3.13, the k_1 and k_2 parametric images with high spatial regularization provides worse estimation than the parametric images with medium and low spatial regularization. Moreover, k_3 and k_4 parametric images with medium spatial regularization gives the best estimation to the original image.

One of the error metrics used to compare the various spatial regularization techniques on parametric image is the Mean Square Error (MSE). MSE is generally used for measuring the image quality. It has a common usage because of being simple for calculating clear physical meaning. The MSE is the cumulative squared error between the estimated and the original image. Algorithms are evaluated based on their performance of estimating the kinetic parameters. MSE is used to evaluate the accuracy of TACs estimated by the algorithm.

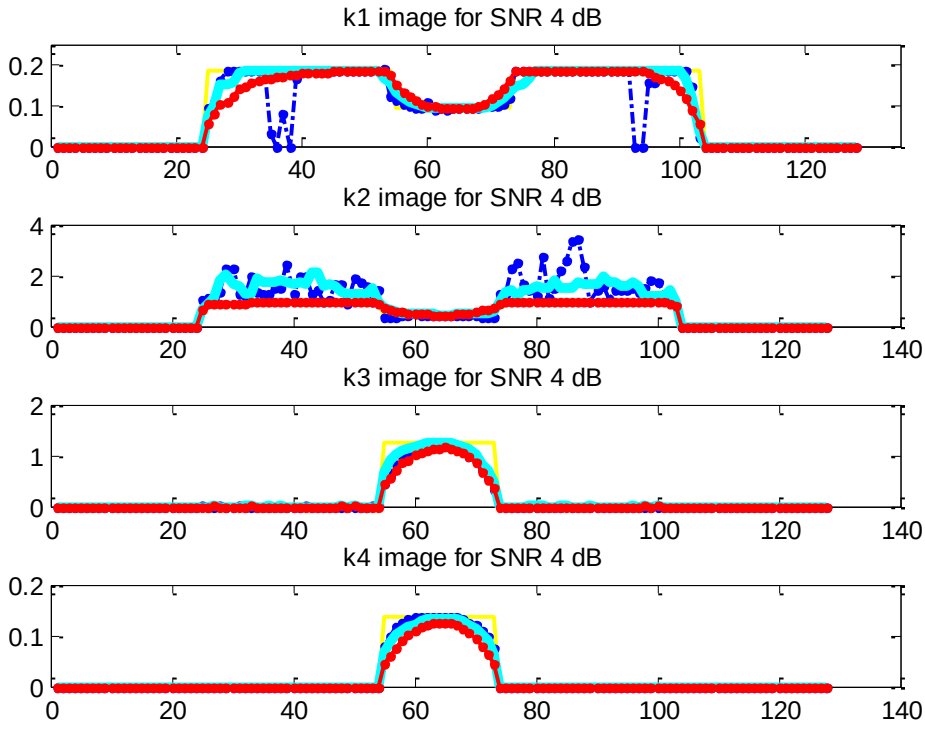

Figure 3.10: Profile of 64th row obtained parametric images with different spatial regularization for 4 dB SNR. Parametric images with original, LR, MR and HR are plotted using yellow, blue, cyan and red colors respectively

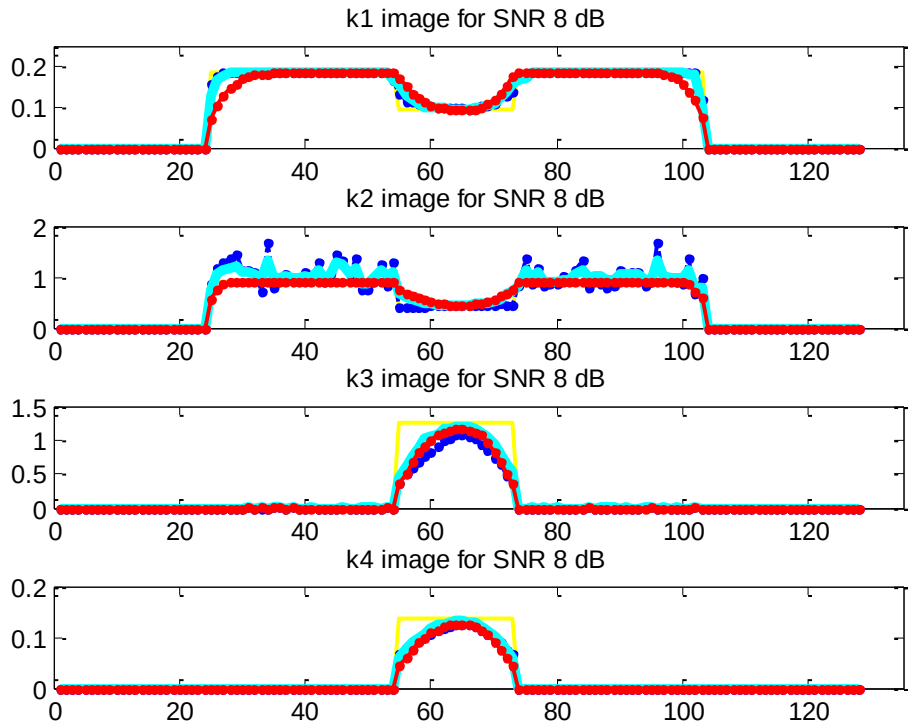

Figure 3.11: Profile of 64th row obtained parametric images with different spatial regularization for 8 dB SNR. Parametric images with original, LR, MR and HR are plotted using yellow, blue, cyan and red colors respectively

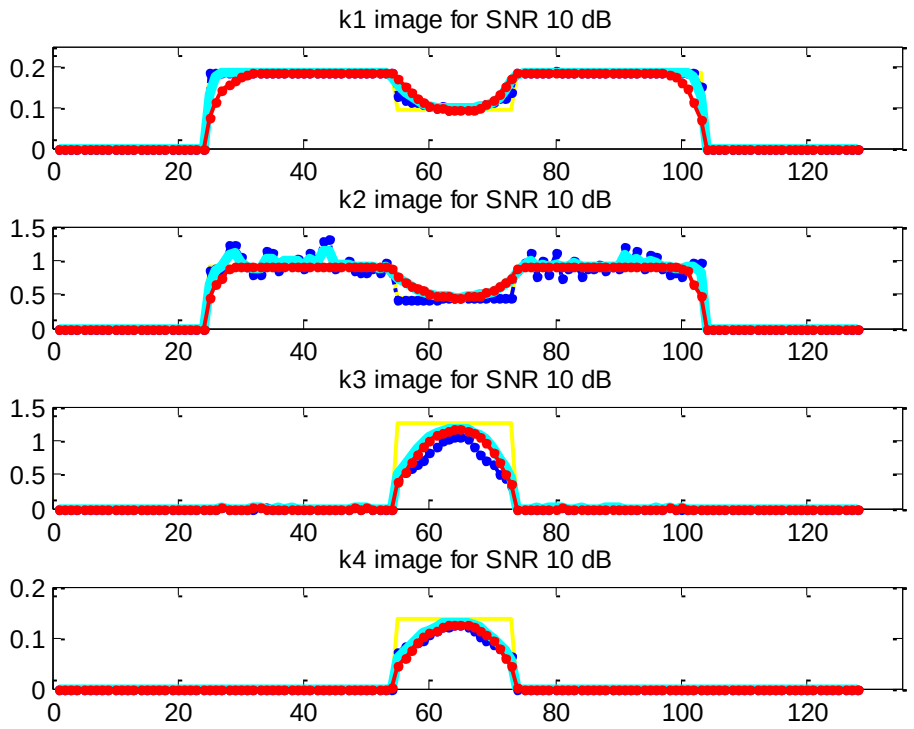

Figure 3.12: Profile of 64th row obtained parametric images with different spatial regularization for 10 dB SNR. Parametric images with original, LR, MR and HR are plotted using yellow, blue, cyan and red colors respectively

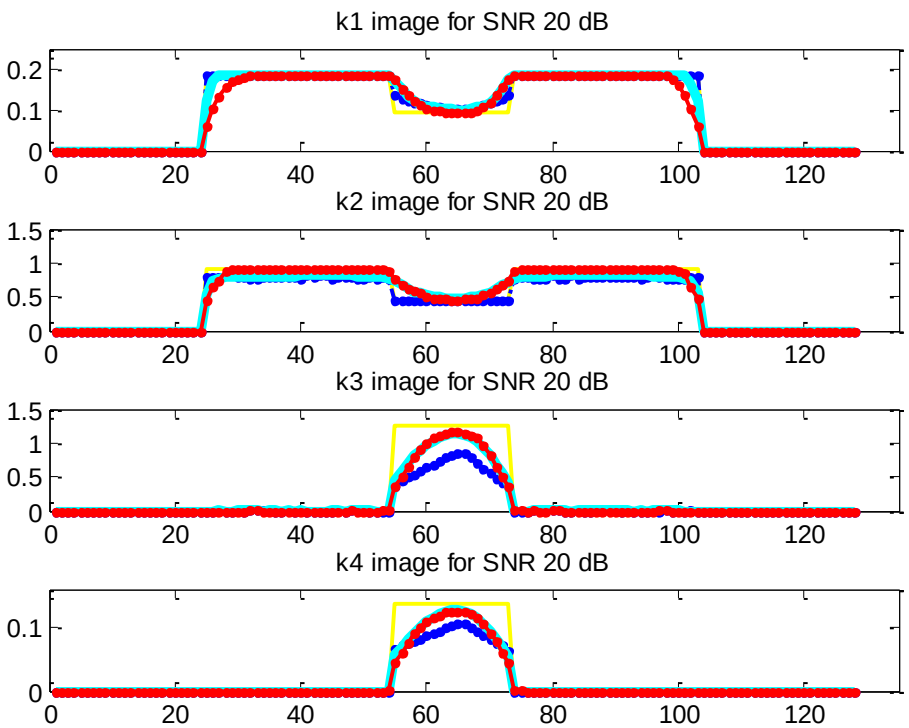

Figure 3.13: Profile of 64th row obtained parametric images with different spatial regularization for 20 dB SNR. Parametric images with original, LR, MR and HR are plotted using yellow, blue, cyan and red colors respectively

We have shown that the optimum estimated parameter images depend on the size, activity distribution of the ROI and spatial regularization parameters. Figure 3.14-3.17 are shown MSE comparison between the various spatial regularization parameters. The error between the original and reconstructed image sequences is plotted as a function of SNR values in a simulated dynamic phantom image. At lower bar plot are shown the minimum error between the original and estimated results.

We study to find a set of spatial regularization parameters that minimize the MSE of the estimated kinetic parameters. In Figure 3.14, mean square errors for the k_1 parametric image with LR, MR and HR spatial regularization are evaluated and plotted.

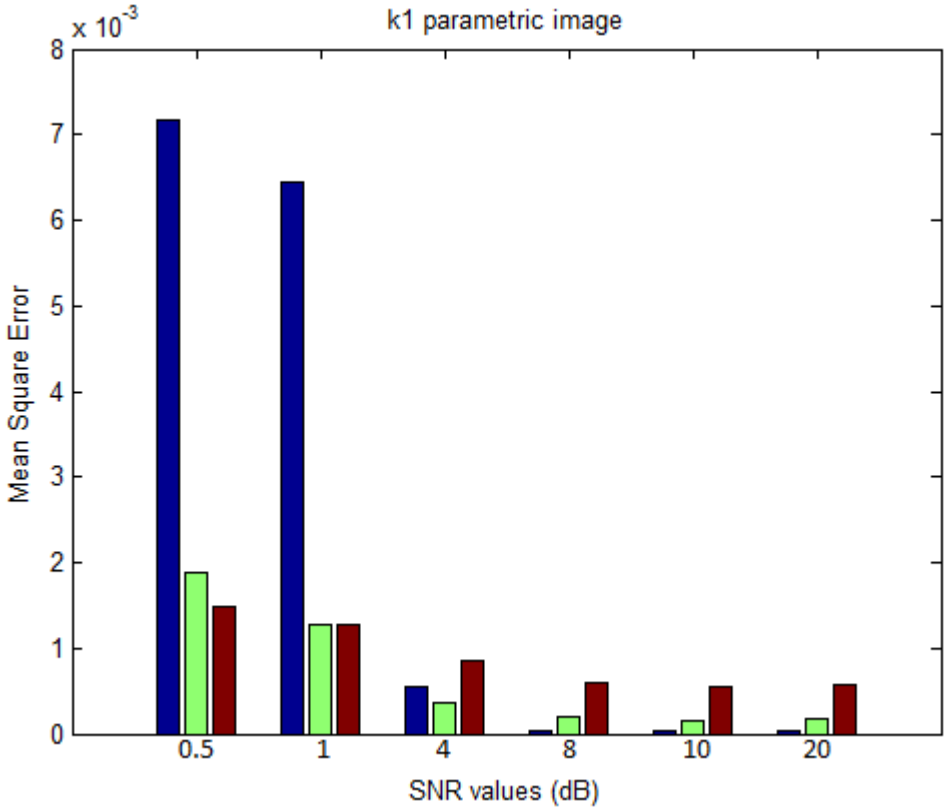

Figure 3.14: Comparison of the Mean Square Error Analysis for k_1 image with different spatial regularization and SNR values. Parametric images with LR, MR and HR are plotted using blue, cyan and red colors respectively.

MSE of the k_1 parametric image with NR is significantly more when it is compared to other spatial regularizations so NR is not plotted. Parametric images with LR, MR and HR are plotted using blue, cyan and red colors, respectively. The k_1 parametric image has high MSE with low regularization parameters for low SNR values. Other

regularization parameters give comparable MSE in the parametric image. This figure demonstrates that, using either HR or MR, the MSE is minimized when the more noise is applied. When SNR values are increased, the MSE is minimized parametric image with using low spatial regularization are chosen to give best estimation results.

Mean square errors for the k_2 parametric image with LR, MR and HR spatial regularization are evaluated and plotted as shown in the Figure 3.15. Parametric images with LR, MR and HR are showed with blue, cyan and red colors respectively. This figure shows that the errors of the kinetic parameter monotonically reduce as the regularization parameter increases when SNR values changed from 0.5 dB to 10 dB. MSE is observed to be relatively insensitive to the high SNR values. In other words, this figure shows that the MSE of the parametric image with different regularization parameters are obtained similar results when less noise is applied. In this case, parametric images having the high SNR values are selected using the appropriate regularization parameter values.

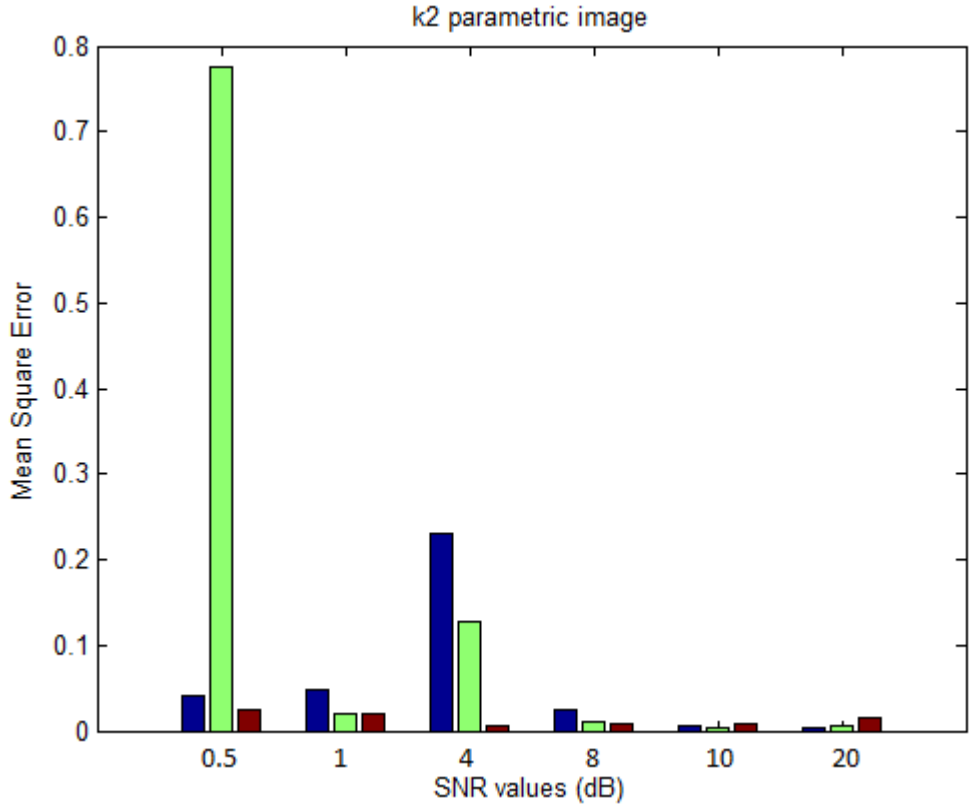

Figure 3.15: Comparison of the Mean Square Error Analysis for k_2 image with different spatial regularization and SNR values. Parametric images with LR, MR and HR are plotted using blue, cyan and red colors respectively.

MSE of k_3 parametric image are plotted as a function of noise levels in Figure 3.16. This figure shows the comparison of the mean square error values in parametric images with various spatial regularization parameters. The error bars of LR, MR and HR results are showed with blue, cyan and red colors respectively. We can see that MR has a good effect on MSE results for all SNR values. In addition, k_3 parametric image has a small region of interest. Therefore, MR provides slightly better results than the other spatial regularization parameters for small ROI.

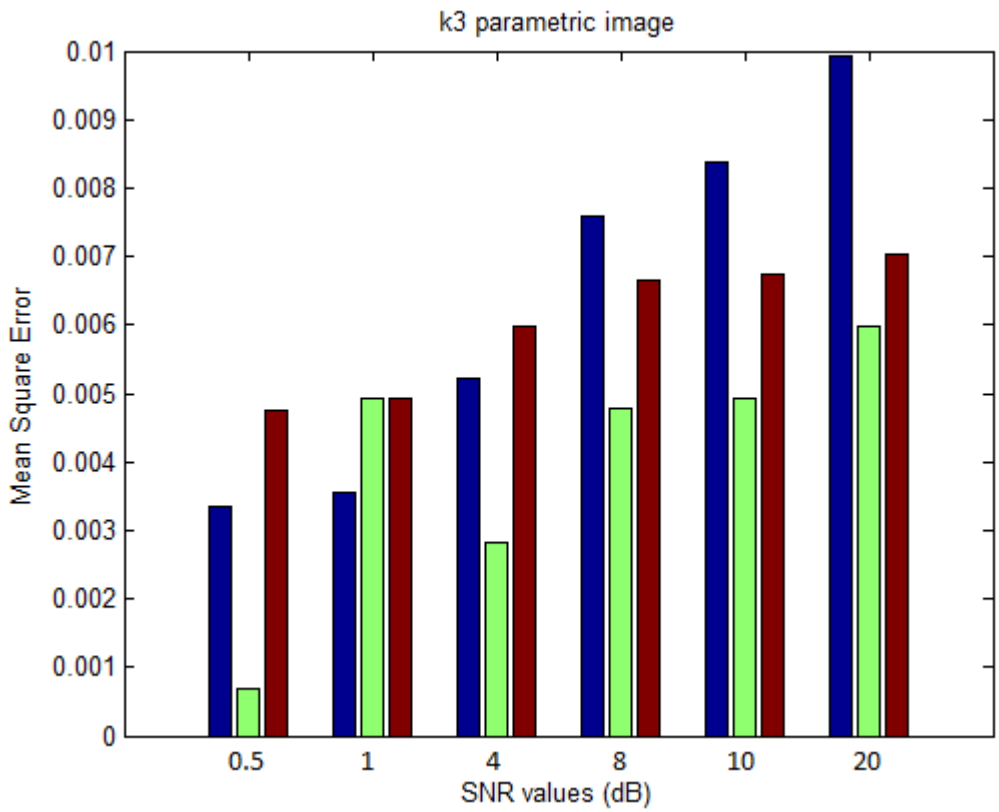

Figure 3.16: Comparison of the Mean Square Error Analysis for k_3 image with different spatial regularization and SNR values. Parametric images with LR, MR and HR are plotted using blue, cyan and red colors respectively.

MSE results of another kinetic parameter image having small region of interest are compared in Figure 3.17. This figure demonstrates the mean square error of the four parameters between the original images and estimated parameter images with different spatial regularization. The optimum regularization parameter for the k_4 parametric image is low spatial regularization parameter. This figure shows that the errors of the kinetic parameter monotonically increase as the regularization parameter increases. Therefore, error is minimum value when it is applied with a low regularization.

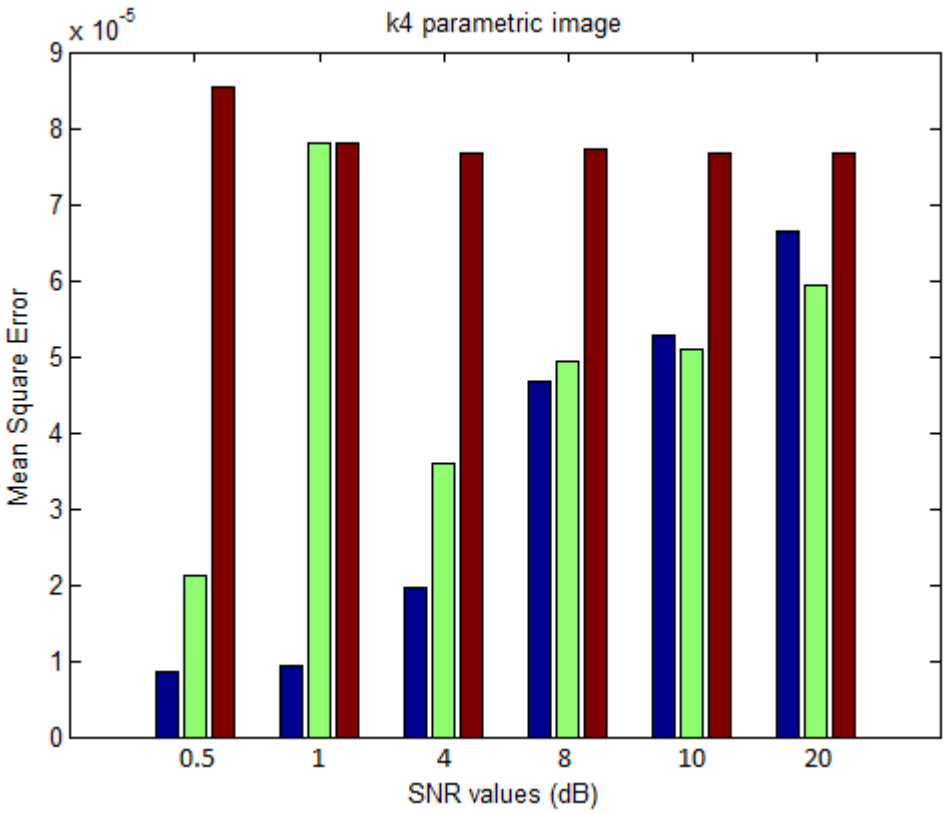

Figure 3.17: Comparison of the Mean Square Error Analysis for k_4 image with different spatial regularization and SNR values. Parametric images with LR, MR and HR are plotted using blue, cyan and red colors respectively.

We compare the mean squared error of the kinetic parameter estimates with the original parametric images and with the estimated parametric images. Tests using parametric images show that we can simultaneously estimate the kinetic parameters of the two tissue compartment model. The MSE of the kinetic parameters increased for some spatial regularization parameters and remained same or decreased for other spatial regularization parameters. Therefore, the values of the optimum regularization parameter are different for kinetic parameters. These results demonstrate the importance of using an appropriate regularization parameter when selecting kinetic parameters.

Since the MSE decomposes into a sum of the bias and variance of the estimator, both quantities are important and need to be as small as possible to achieve good estimation performance. Phantom image has two different circular regions of interest and ROI 1 stands for region of interest with large radius whereas ROI 2 stands for region of interest with small radius in this thesis. The bias and coefficient of variance are expressed in terms of percentage as follows

$$Bias(\%) = 100 \times \left(\frac{\bar{\hat{\theta}} - \bar{\theta}}{\bar{\theta}}\right) \quad \textbf{(3.1)}$$

$$Coefficient\ of\ Varience(\%) = 100 \times \left(\frac{\sigma}{\bar{\hat{\theta}}}\right) \quad \textbf{(3.2)}$$

where $\bar{\theta}$ denotes mean of the original image, $\bar{\hat{\theta}}$ is an estimate of $\bar{\theta}$ made by averaging over the pixels with in the ROI's in the reconstructed image. The coefficient of variation (CV) represents the ratio of the standard deviation (σ) to the mean. By calculating the bias and variance of ROI activity quantification with kinetic modeling, we can analyze how regularization in image reconstruction affects kinetic parameter estimation.

Approximate expressions for the bias, coefficient of variance, and mean squared error of the estimated parametric images have been derived, which provide guidance for selecting a proper regularization parameter. Table 3.1 shows these values for ROI 2 of the k_1 parametric image and estimated parametric images with NR, LR, MR and HR when different SNR values are applied.

Table 3.1: Results of Bias, CV and MSE for ROI 2 of k_1 parametric images with different spatial regularization

k1	**NR**			**LR**		
SNR (dB)	**Bias (%)**	**CV (%)**	**MSE (ROI 2)**	**Bias (%)**	**CV (%)**	**MSE (ROI 2)**
0.5	3.37	68.50	9.8×10^{-3}	0.08	5.65	6.1×10^{-5}
1	1.66	73.73	1.2×10^{-2}	0.98	5.47	5.6×10^{-5}
4	14.11	78.39	1.3×10^{-2}	6.34	8.03	1.8×10^{-4}
8	67.31	66.55	1.2×10^{-2}	23.21	11.05	6.7×10^{-4}
10	72.62	53.96	9.1×10^{-3}	28.27	12.24	8.6×10^{-4}
20	91.08	24.79	8.5×10^{-3}	34.1	11.15	1.2×10^{-3}
k1	**MR**			**HR**		
SNR (dB)	**Bias (%)**	**CV (%)**	**MSE (ROI 2)**	**Bias (%)**	**CV (%)**	**MSE (ROI 2)**
0.5	2.69	8.17	1.4×10^{-4}	22.84	15.55	8.3×10^{-4}
1	29.04	18.45	1.2×10^{-3}	29.04	18.45	1.2×10^{-3}
4	16.65	14.96	6.5×10^{-4}	35.96	20.22	1.6×10^{-3}
8	31.65	21.11	1.5×10^{-3}	45.51	24.93	2.3×10^{-3}
10	35.34	21.52	1.8×10^{-3}	45.6	25.17	2.4×10^{-3}
20	43.35	25.08	2.6×10^{-3}	48.41	26.96	2.8×10^{-3}

Since the area of ROI 2 is smaller, difference between estimated and original values is less. Therefore, when SNR values increase, bias of k_1 parametric images with NR, LR, MR, HR also increase for ROI 2. MSE of parametric images with different spatial regularizations also prove that bias and coefficient of variance results are correct. We expect that bias values of parametric image with LR to be less than HR and MR which can be shown also in our results. Normally, variance is increase as the regularization parameter decreases but due to under regularization effect of the parametric image with LR, coefficient of variance is found less than other regularizations. In other words, the edges of parametric image generate a large variation at these high regularization levels.

Bias, CV and MSE are calculated for ROI 2 of the k_2 parametric images with NR, LR, MR and HR and results are shown in Table 3.2. When SNR values increase, bias of k_2 parametric image with LR decrease for ROI 2 as expected. Bias of the k_2 parametric images with HR is calculated approximately similar for different SNR values.

Table 3.2: Results of Bias, CV and MSE for ROI 2 of k_2 parametric images with different spatial regularization

k2	**NR**			**LR**		
SNR (dB)	**Bias (%)**	**CV (%)**	**MSE (ROI 2)**	**Bias (%)**	**CV (%)**	**MSE (ROI 2)**
0.5	81	110.74	3.6×10^{-1}	7.67	15.23	1.3×10^{-2}
1	68.8	119.09	4.3×10^{-1}	9.88	15.32	1.3×10^{-2}
4	23.5	123.29	5.0×10^{-1}	16.12	8.82	8.8×10^{-3}
8	89.94	107.50	4.5×10^{-1}	4.55	4.38	1.5×10^{-3}
10	86.39	101.33	3.6×10^{-1}	3.83	3.23	7.8×10^{-4}
20	100	44.44	3.0×10^{-1}	2.38	0.57	1.4×10^{-4}
k2	**MR**			**HR**		
SNR (dB)	**Bias (%)**	**CV (%)**	**MSE (ROI 2)**	**Bias (%)**	**CV (%)**	**MSE (ROI 2)**
0.5	15.11	15.31	1.6×10^{-2}	39.42	26.07	5.4×10^{-2}
1	40.50	24.64	5.2×10^{-2}	40.50	24.64	5.2×10^{-2}
4	15.87	16.71	1.8×10^{-2}	36.90	18.63	3.5×10^{-2}
8	23.85	15.50	2.1×10^{-2}	39.81	18.44	3.7×10^{-2}
10	29.86	15.69	2.6×10^{-2}	38.92	17.98	3.6×10^{-2}
20	36.68	16.36	3.3×10^{-2}	39.53	17.43	3.6×10^{-2}

Bias, coefficient of variance and mean squared error of the estimated k_3, k_4 parametric images with various spatial regularizations for ROI 2 are calculated and are listed in Table 3.3 and Table 3.4. These statistics values of the these parametric images with HR is calculated approximately similar for different SNR values.

Table 3.3: Results of Bias, CV and MSE for ROI 2 of k_3 parametric images with different spatial regularization

k3	**NR**			**LR**		
SNR (dB)	**Bias (%)**	**CV (%)**	**MSE (ROI 2)**	**Bias (%)**	**CV (%)**	**MSE (ROI 2)**
0.5	96.89	50.82	1.34	9.67	20.03	1.7×10^{-1}
1	94.17	56.79	1.33	13.17	20.35	1.8×10^{-1}
4	76.36	53.09	1.21	32.45	20.27	2.8×10^{-1}
8	62.34	30.17	0.78	51.57	15.09	4.1×10^{-1}
10	59.03	22.96	0.64	54.99	14.12	4.6×10^{-1}
20	55.44	4.46	0.47	60.29	9.56	5.4×10^{-1}
k3	**MR**			**HR**		
SNR (dB)	**Bias (%)**	**CV (%)**	**MSE (ROI 2)**	**Bias (%)**	**CV (%)**	**MSE (ROI 2)**
0.5	4.74	9.36	3.5×10^{-2}	37.92	15.77	2.6×10^{-1}
1	37.66	16.43	2.7×10^{-1}	37.66	16.43	2.7×10^{-1}
4	23.86	15.88	1.5×10^{-1}	43.64	17.72	3.3×10^{-1}
8	38.33	17.00	2.6×10^{-1}	47.15	19.01	3.6×10^{-1}
10	39.51	16.34	2.7×10^{-1}	46.51	19.04	3.7×10^{-1}
20	44.41	16.11	3.2×10^{-1}	48.15	19.55	3.8×10^{-1}

ROI delineation of functional regions is a tedious, time-consuming, and error-prone task. Moreover, these delineations may vary depending on the quality of the PET image data. The quantitative accuracy and precision of the reconstructed ROI value was examined for two different ROI sizes and four different spatial regularization.

Kinetic parameters k_1, k_2, k_3 and k_4 are 0.1836, 0.8968, 0 and 0 for the ROI 1 with bigger radius whereas k_1, k_2, k_3 and k_4 are 0.3918, 0.4484, 1.2408 and 0.1363 for the ROI 2 with small radius. Therefore, bias, variance and MSE values are calculated for only k_1 and k_2 parametric images. Table 3.5 and Table 3.6 show these values for ROI 1 of the k_1 and k_2 parametric images and estimated parametric images with NR, LR, MR and HR when different SNR values are applied. The results show that both bias and variance improve rapidly as the ROI size increases.

Table 3.4: Results of Bias, CV and MSE for ROI 2 of k_4 parametric images with different spatial regularization

k4	NR			LR		
SNR (dB)	**Bias (%)**	**CV (%)**	**MSE (ROI 2)**	**Bias (%)**	**CV (%)**	**MSE (ROI 2)**
0.5	82.29	49.34	7.1×10^{-2}	0.01	9.33	4.6×10^{-4}
1	76.43	47.62	5.9×10^{-2}	0.15	9.63	4.7×10^{-4}
4	66.03	23.82	8.8×10^{-3}	13.91	13.21	1.0×10^{-3}
8	60.4	20.74	1.3×10^{-2}	35.30	10.95	2.5×10^{-3}
10	58.08	16.50	8.3×10^{-3}	39.68	10.72	2.8×10^{-3}
20	58.82	3.55	6.4×10^{-3}	44.45	7.26	3.5×10^{-3}
k4	**MR**			**HR**		
SNR (dB)	**Bias (%)**	**CV (%)**	**MSE (ROI 2)**	**Bias (%)**	**CV (%)**	**MSE (ROI 2)**
0.5	19.89	11.18	1.1×10^{-3}	45.81	19.25	4.6×10^{-3}
1	44.41	18.19	4.2×10^{-3}	44.41	18.19	4.2×10^{-3}
4	26.36	14.39	1.9×10^{-3}	44.03	17.86	4.2×10^{-3}
8	35.69	14.96	2.6×10^{-3}	44.35	17.69	4.2×10^{-3}
10	36.08	14.82	2.7×10^{-3}	44.14	17.72	4.1×10^{-3}
20	40.87	14.54	3.2×10^{-3}	44.37	17.62	4.1×10^{-3}

Table 3.5: Results of Bias, Variance and MSE for ROI 1 of k_1 parametric image

k1	NR			LR		
SNR (dB)	**Bias**	**Variance**	**MSE (ROI 1)**	**Bias**	**Variance**	**MSE (ROI 1)**
0.5	0.01	0.60	0.73	0.17	0.03	2.5×10^{-2}
1	0	0.64	0.86	0.15	0.04	2.2×10^{-2}
4	0.60	0.75	1.56	0	0.02	1.9×10^{-3}
8	0.49	0.61	1.22	0	0.004	1.0×10^{-4}
10	0.41	0.38	0.60	0	0.002	3.0×10^{-5}
20	0.43	0.11	0.20	0	0.001	1.0×10^{-5}
k1	**MR**			**HR**		
SNR (dB)	**Bias**	**Variance**	**MSE (ROI 1)**	**Bias**	**Variance**	**MSE (ROI 1)**
0.5	0.003	0.06	6.5×10^{-3}	0.02	0.05	5.1×10^{-3}
1	0.02	0.04	4.4×10^{-3}	0.02	0.04	4.4×10^{-3}
4	0	0.02	1.3×10^{-3}	0.01	0.03	2.8×10^{-3}
8	0	0.01	6.0×10^{-4}	0	0.03	1.9×10^{-3}
10	0	0.01	4.1×10^{-4}	0	0.03	1.7×10^{-3}
20	0	0.01	4.8×10^{-4}	0	0.03	1.8×10^{-3}

Table 3.6: Results of Bias, Variance and MSE for ROI 1 of k_2 parametric image

k2	NR			LR		
SNR (dB)	**Bias**	**Variance**	**MSE (ROI 1)**	**Bias**	**Variance**	**MSE (ROI 1)**
0.5	0.69	2.46	9.83	0.06	0.22	1.4×10^{-1}
1	1.77	2.42	10.64	0.01	0.26	1.7×10^{-1}
4	2.95	1.72	11.46	0.52	0.48	8.0×10^{-2}
8	2.02	1.18	5.94	0.11	0.18	8.5×10^{-2}
10	1.74	0.95	3.85	0.01	0.11	2.3×10^{-2}
20	1.77	0.44	2.99	0.11	0.01	1.3×10^{-2}
k2	**MR**			**HR**		
SNR (dB)	**Bias**	**Variance**	**MSE (ROI 1)**	**Bias**	**Variance**	**MSE (ROI 1)**
0.5	1.77	0.70	2.69	0.28	0.11	7.9×10^{-2}
1	0.25	0.10	6.4×10^{-2}	0.25	0.10	6.4×10^{-2}
4	0.63	0.25	4.5×10^{-2}	0.06	0.08	1.9×10^{-2}
8	0.11	0.11	3.8×10^{-2}	0	0.09	2.4×10^{-2}
10	0.02	0.07	1.3×10^{-2}	0	0.11	3.0×10^{-2}
20	0.09	0.05	2.2×10^{-2}	0.04	0.14	4.8×10^{-2}

4. DISCUSSION

The quantitative accuracy and precision of the reconstructed parametric images are examined for two different ROI sizes, six various noise level and four different spatial regularization. Bias, CV and MSE are calculated at two different ROI areas of the parametric images with NR, LR, MR and HR for SNR values. MSE of parametric images with different spatial regularizations and SNR levels prove that bias and coefficient of variance results are correct for ROI 1 and ROI 2.

Noise based estimation error (NEE) is the estimation error when no spatial regularization is applied to the parametric images and is caused only by the added noise. Regularization based estimation error (REE) is due to the applied spatial regularization to the parametric images.

For optimum case of REE and NEE; when REE is increased, NEE is extremely decreased. When region of interest size is decreased, NEE is slightly decreased. Parametric images with different spatial regularizations prove that bias and coefficient of variance results are correct. We expect that REE values of parametric image with large region to be less than small region which can be shown also in our results. Parameter images having big region of interest result aproximately same as the optimum case. However, parameter images having small region of interest result different and when REE is increased, NEE is slightly decreased. That is why bias and MSE increase with SNR levels.

Coefficient of variance is increased as the amount of regularization is increased due to over regularization effect. Since parametric image with LR is the most under regularization effect of the parametric image, coefficient of variance is less than the other regularizations.

Optimization of regularization parameter for four different parameter is a hand task. Results of parametric images using different regularization levels obtained with different levels of noise and various region of area demonstrate the importance of the choice of an appropriate regularization parameter.

Bias and CV of the k_2, k_3, k_4 parametric images with high spatial regularization is calculated approximately similar MSE when SNR values changes for ROI 2. This is because of the fact that the total estimation error is dominated by REE as NEE is limited effect of parametric images with high spatial regularization. Hence, only little changes in bias and CV are observed at HR. On the other hand, MSE changes drastically for low spatial regularization when SNR is changed. This is because of the fact that the total estimation error is dominated by NEE whereas REE is limited. REE effect of parametric images with high spatial regularization for ROI 1 is not as high as for ROI 2 due to the over smoothing of edges.

The regularization parameter should be chosen depending on the SNR and region of interest size. If the parametric images have small region of interest, low regularization parameter should be chosen because estimation error is dominated by REE. On the other hand, for parametric images having large region of interest, high regularization parameter should be chosen since estimation error is dominated by NEE. Therefore, adaptive regularization should be preferred. This method should change the level of regularization as a function of ROI and different level of noise.

5. CONCLUSION

Positron emission tomography (PET) is a useful diagnostic tool due to its ability to image biological functions in vivo. PET imaging has several advantages such as high sensitivity and ability for quantitative measurement. Unlike other imaging modalities, dynamic PET data suffers from leading to poor signal to noise ratios. This causes difficulties in the solution of the low SNR problem for estimation of the parameters. In this work the effects of kinetic parameter estimation on spatial regularization are investigated for the parametric images which are constructed with different SNR values.

In this thesis, the phantom image which has two various regions of interest is constructed by using MATLAB program. We used 11C Racloride as a tracer to detect dopamine release during processing of executive inhibition. Quantification of tracer kinetics using dynamic PET provides important information for understanding the physiological and biochemical processes in humans. It is often necessary to analyze the time response of a tracer. The time activity curve is obtained by sampling the images in ROI's and used to estimate tracer kinetic parameters based on a compartmental model. The compartmental model is a basic concept to quantitatively evaluate PET data. PET imaging has focused on two different regions of interest other than background studies. Four different original images are developed according to kinetic parameters taken from the literature. We have demonstrated that it is possible to estimate kinetic parameters k_1, k_2, k_3, and k_4.

The selection of the regularization parameter is an important issue in the parameter estimation for dynamic PET. The regularization parameter should be chosen depending on the size of the ROI, REE and NEE. For example, if the parametric images have small region of interest, low regularization parameter should be chosen because estimation error is dominated by REE.

In our simulation, which uses a phantom image, the estimated parametric images were close to the original parametric images. For comparison of the parametric

images, bias, coefficient of variance and mean squared error values are calculated. These values of the parameter images have been derived as a function of the regularization parameters and various noise levels. In addition, some of the estimated kinetic parameters have higher MSE, some of them have either similar or lower MSE.

We use the L2 norm as the similarity metric between TACs and need to investigate the performance of other estimators including Huber, Tukey, Cauchy. In future, the compartmental model will play an important role in molecular imaging. Further simulations and tests with real data are needed to analyze the MSE, bias, and variance of the kinetic parameter estimations. In addition, adaptive regularization should be preferred to analyze these results.

REFERENCES

[1] **Phelps, M., Mazziotta, J. C., and Schelbert, H. R.** (1986), Positron Emission Tomography and Autoradio graphy: Principles and Applications for the Brain and Heart, *Raven Press*, New York.

[2] **Inki Hong, M.C., Sanghee Cho, C. Michel.** (2011) Complementary reconstruction: improving image quality in dynamic PET studies, in: *Proceedings IEEE Nuclear Science Symposium*, pp. 4327–4328

[3] **Saad, A., Smith, B., Hamarneh, G., and Moller, T.** (2007) Simultaneous segmentation, kinetic parameter estimation, and uncertainty visualization of dynamic PET images., in: *Proceedings of International Conference on Medical Image Computing and Computer Assisted Intervention*, Brisbane, Australia.

[4] **Qi, J., and Huessman, R.** (2006). Theoretical study of penalized-likelihood image reconstruction for region of interest quantification, *IEEE Transactions on Medical Imaging*, 25(5) 640–648

[5] **Fessler, J.A., and Rogers, W.L.** (1996). Spatial resolution properties of penalized likelihood image reconstruction: Space-invariant tomographs, *IEEE Transactions on Image Processing*, vol. 5, no. 9, pp. 1346–1358, Sep.

[6] **Coxson, P. C., Huesman, R. H., and Borland, L.** (1997). Consequences of using a simplified kinetic model for dynamic PET data, J. *Nucl. Med*., vol. 38, no. 4, pp. 660–667.

[7] **Chen, K., Huang, S. C., and Yu, D. C.** (1991). The effects of measurement errors in the plasma radioactivity curve on parameter estimation in positron emission tomography, *Phys. Med. Biol.*, vol. 36, no. 9, pp. 1183–1200.

[8] **Wang, G., and Qi, J.** (2009). Analysis of penalized likelihood image reconstruction for dynamic PET quantification, *IEEE Transactions on Medical Imaging*, 28 (4),608–620.

[9] **Kamasak, M. E.** (2014). Effects of spatial regularization on kinematic parameter estimation for dynamic PET. *Biomedical Signal Processing and Control Imaging*, 9, 6-13.

[10] **Webb, A.** (2003). Introduction to Biomedical Imaging, *Wiley Interscience IEEE Press* , Hoboken, NJ.

[11] **Huang, S.C., Phelps, M., Homan, E., Sideris, K., Selin, C., and Kuhl, D.** (1980). Non-invasive determination of lo cal cerebral metabolic rate of glucose in man, *Am. J. Physiol*., p.E69.

[12] **Rahmim, A, Cheng J.C., Blinder, S., Camborde, M.L., and Sossi, V**. (2005). Statistical dynamic image reconstruction in state of the art high resolution PET. *Phys Med Bio*; 50:4887–4912.

[13] **Rahmim, A., and Zaidi, H.** (2008). PET versus SPECT: strengths, limitations and challenges, *Nuclear medicine communications*.

[14] **Nichols, T.E., Qi, J., Asma, E., and Leahy, R.M.** (2002). Spatiotemporal reconstruction of list mode PET data. *IEEE Transactions on Medical Imaging*; 21:396–404

[15] **Barber, D.C.** (1980). The use of principal components in the quantitative analysis of gamma camera dynamic studies. *Phys. Med. Biol*. 25, 283–292.

[16] **Kamasak, M.E., and Bayraktar, B.** (2006). Unsupervised clustering of dynamic PET images on the projection domain. *Proceedings of the SPIE Medical Imaging*, pp. 1539–1548.

[17] **Kamasak, M.E., Bouman, C.A., Morris, E.D., and Sauer, K.** (2005). Direct reconstruction of kinetic parameter images from dynamic PET data, *IEEE Transactions on Medical Imaging*, 24 (5) 636–650.

[18] **Koeppe, R.A., Frey, K.A., Snyder, S.E., Meyer, P.,Kilbourn, M.R., Kuhl, D.E.** (1999). Kinetic modeling of N-[11C] methylpiperidin-4-yl propionate: alternatives for analysis of an irreversible positron emission tomography trace for measurement of acetylcholinesterase activity in human brain. *J Cereb Blood Flow Metab*., 19:1150-1163

[19] **Farde, L., Eriksson, L., Blomquist, G., and Halldin, C.** (1989). Kinetic analysis of central [11C] raclopride binding to D2-dopamine receptors studied by PET a comparison to the equilibrium analysis. *J Cereb Blood Flow Metab*. 9:696-708.

[20] **Carson, R. E., and Lange, K.** (1985). The EM parametric image reconstruction algorithm, *Journal of the American Statistical Association*, vol. 80, no. 389, pp. 20–22.

[21**] Jeffrey Fessler, A.** (1996). Mean and variance of implicitly de-fined bias estimators (such as penalized maximum likeli-hood): applications to tomography, *IEEE Transactions on Image Processing*, vol. 5, no. 3, pp. 493–506, March.

[22] **Qi, J., and Huessman, R.** (2006). Theoretical study of penalized-likelihood image reconstruction for region of interest quantification, *IEEE Transactions on Medical Imaging*, vol.25, no. 5, pp. 640–648.

[23] **Wang, G., and Qi, J.** (2009).“Analysis of penalized likelihood image reconstruction for dynamic PET quantification”, *IEEE Transactions on Medical Imaging*, vol. 28, no. 4, pp. 608–620.

[24] **Kamasak, M.E.**, **Bouman, C.A., Morris, E.D., and Sauer, K.** (2005). Reconstruction of kinetic parameter images directly from dynamic PET sonograms. *IEEE Transactions on Medical Imaging*, vol.24, no. 5, pp. 636–650.

[25] **Wack, D.S., Badgaiyan, R.D.** (2011), Complex singular value decomposition based noise reduction of dynamic PET images, *Current Medical Imaging Reviews 7*, pp. 113–117

[26] **Kao, C.M., Yap, J.T., Mukherjee J., Wernick, M.** (1997), Image reconstruction for dynamic PET based on low-order approximation and restoration of the sinogram, *IEEE Transactions on Medical Imaging*, vol. 16, no. 6, pp. 738–749.

[27] **Wernick, M.N. Infusino, E.J., Milosevic, M.** (1999), Fast spatio temporal image reconstruction for dynamic PET, *IEEE Transactions on Medical Imaging*, vol.18, no.3, pp. 185–195.

[28] **Wong, K.P., Feng, D., Meikle, S.R., Fulham, M.J.** (2001), Simultaneous estimation of physological parameters and the input function - in vivo PET data, *IEEE Transactions on Information Technology in Biomedicine*, vol.5, no.1, pp. 67–76.

[29] **PET-Schema** (2005). In *Wikipedia*. Date retrieved: 07.03.2014, adress: http://en.wikipedia.org/wiki/File:PET-schema.png

CURRICULUM VITAE

Name Surname: Sahra Alak

Place and Date of Birth: Balikesir/Turkey-22/06/1987

Address: Istanbul/Turkey

E-Mail: sahralak@gmail.com

B.Sc.: Electrical-Electronics Engineering Department, Yeditepe University

Industrial and Systems Engineering Department, Yeditepe University

Professional Experience and Rewards:

- Tubitak Domestic General Graduate Scholarship
- 1st Degree of Electrical-Electronics Engineering Department at Yeditepe University